A COMPARISON OF HYDROGEN AND MERCURY EMBRITTLEMENT OF NICKEL BASED ALLOYS

By

LELAND BRUCE TRAYLOR

Bachelor of Science in Mechanical Engineering

Oklahoma State University

Stillwater, Oklahoma

1982

Submitted to the Faculty of the Graduate College
of the Oklahoma State University
in partial fulfillment of the requirements
for the Degree of
MASTER OF SCIENCE
July, 1983

A COMPARISON OF HYDROGEN AND MERCURY EMBRITTLEMENT OF NICKEL BASED ALLOYS

Thesis Approved:

C E Price
Thesis Adviser

R L Lowery

B. Kottcamp

Norman N Durham
Dean of Graduate College

ACKNOWLEDGMENTS

I would like to express my deepest appreciation to my major adviser, Dr. C. E. Price, whose guidance, advice and genuine concern made this thesis possible. I would also like to thank Keith Good and Dr. Bilgin Kaftanoglu, who have provided many helpful suggestions and advise.

A scholarship, provided by Conoco, has helped make my graduate education possible and is acknowledged with gratitude. I would also like to thank the Department of Mechanical Engineering, Oklahoma State University, for providing assistantships, which have helped tremendously.

A special thanks goes to TRW Reda Pump Company for providing materials for this project.

Finally, I would like to thank my wife, Sherri, for her devotion, encouragement and many sacrifices.

TABLE OF CONTENTS

LIST OF TABLES

LIST OF FIGURES

CHAPTER I

INTRODUCTION

A. The Importance of Hydrogen Embrittlement

Environmentally assisted cracking of engineering materials is a serious problem that limits the reliability of engineering structures operating in hostile environments. This year, environmentally assisted cracking will cause thousands of failures and large losses of life and property. Also, material limitations are the major barrier in the way of solving some of this nation's problems, not the least of which is energy production. In recent years, it has become economically possible to produce oil and gas from deeper and more corrosive wells. To combat corrosion and environmentally assisted cracking, more expensive nickel base alloys have been replacing alloy steels for this service.[1,2] In the refining industry, higher temperatures and more hostile environments are encountered during processing of lower grade feedstocks, which leads to the use of nickel based alloys.[3] In general, more structures are operating in hostile environments than ever before, and many are made of nickel base alloys. When a failure of one of these structures can cost millions of dollars or the loss of life, it is clear that an understanding of these problems is very important in order to optimize material selection, design and operating procedure. This thesis will examine two areas of environmentally assisted cracking, hydrogen embrittlement and mercury embrittlement of nickel base alloys.

Hydrogen embrittlement is a general term that refers to the degradation of metals in the presence of hydrogen. The form of the damage could be blisters, cracks or brittle phase formation. The source of the hydrogen could be external or electrochemical. External hydrogen embrittlement is damage that results from a high pressure hydrogen environment, such as NASA and its subcontractors experienced in the mid 1960's when several of its high pressure hydrogen storage tanks failed.[4] Electrochemical sources of hydrogen are mainly the result of corrosive or disassociation reactions, like those that occur during galvanic corrosion or in hydrogen sulfide environments. The conditions that are needed to cause hydrogen embrittlement are a source of atomic hydrogen, a significant tensile stress and a susceptible material. Absorption of hydrogen and thus hydrogen embrittlement is increased by hydrogen evolution poisons, for example sulfur compounds, and by higher temperatures and pressures. These conditions minimize the recombinations of atomic hydrogen to give molecular hydrogen which does not react.

Similar to hydrogen embrittlement, liquid metal embrittlement occurs when a susceptible alloy is exposed to a stress and a liquid metal simultaneously. Although not as industrially important as hydrogen embrittlement, liquid metal embrittlement is a concern in the nuclear power industry where liquid metals are used as heat transfer media. Liquid metal embrittlement is also encountered occasionally in other industrial situations, where it is not well understood. A lack of information about the effect of mercury on nickel base alloys led Price and Good[5] to investigate the mercury embrittlement characteristics of ten nickel based alloys. Their findings indicate that all ten nickel alloys are embrittled to some degree. Their results are interesting

because they suggest that the fracture surface characteristics are similar to those found in hydrogen. Indeed, Hertzberg[6] and others[7] suggest that hydrogen embrittlement, liquid metal embrittlement and stress corrosion cracking may all be due to the same mechanism. There is already some experimental evidence to support this theory. Lynch[8] has done extensive work comparing mercury and hydrogen embrittlement in nickel single crystals, while Speidel[9] has shown a connection between liquid metal embrittlement and stress corrosion cracking.

B. Purpose of Investigation

1. To determine the extent of embrittlement of nickel alloys in the hydrogen and mercury environments under a variety of conditions.

2. To discover and classify the fracture topography to determine similarities and differences between mercury and hydrogen fractures.

3. To document the effects of hydrogen and mercury embrittlement on specific properties in the alloys under differing conditions; to discover how material and environmental conditions affect the extent of embrittlement.

4. From the experimental evidence and the literature, to comment on the implications of this research to environmental assisted cracking mechanisms, materials and testing.

CHAPTER II

LITERATURE SURVEY

A. Introduction

A large amount of literature exists concerning hydrogen embrittlement of high strength steels. Many theories have been proposed to explain these phenomenona in steels. A recent review of the subject is reference 10. For nickel based alloys, however, much less research has been done. Hydrogen embrittlement of nickel alloys, in some ways, is much different than in hydrogen embrittlement of steels. For example, nickel alloys have the face centered cubic (FCC) structure that is closed packed and does not allow diffusion to occur readily while steels have a more open body centered cubic (BCC) structure. In steels, only high strength steels are affected by hydrogen embrittlement while the affect of nickel alloys does not depend on strength levels, because pure nickel single crystals are embrittled. In light of the differences between nickel alloys and high strength steels, it is possible that the embrittlement is not caused by the same mechanism. Lynch,[7] in a recent paper, reviews the 5 prominent theories of hydrogen embrittlement of high strength steel. He contends that these theories are also applicable to hydrogen embrittlement of nickel alloys.

B. Mechanisms of Hydrogen Embrittlement

1. High Pressures at Internal Voids

The idea behind this theory is that atomic hydrogen diffuses through the metal lattice and recombines at discontinuities, such as grain boundaries and second phase particles to form molecular hydrogen, which builds up to large pressures (10^4 MPa).[11] These pressures then assist the crack growth process by increasing the actual stress around the crack tip. This process is responsible for the occurrence of hydrogen blisters in steels and has been shown to be a contributory factor to hydrogen embrittlement in some specific cases.[11] However, for face centered cubic materials, the steady state diffusion rate is too low to account for hydrogen embrittlement more than a fraction of a millimeter deep.[12] Results from a study[13] on Inconel 600 have shown that precharging of the specimens is not needed to cause hydrogen embrittlement, and indeed the amount of precharging is not a very significant variable. Some revisions of this theory have stipulated that vastly increased hydrogen diffusion rates occur during plastic deformation and the voids become pressurized during the necking process. Pressure theories, by themselves, do not explain the very large variations in the amounts of reduction in plasticity between similar alloys. Also, the great similarities between hydrogen embrittlement and liquid metal embrittlement are not well explained by a volume effect theory such as this because liquid metal embrittlement is most likely a surface effect, as will be shown later.

2. Interactions Between Dissolved Hydrogen and Dislocations

Beachem[14] and others[15] observed that in some cases subcritical

crack growth in gaseous hydrogen produced entirely dimpled fracture surfaces, thus they reasoned that the hydrogen facilitated plastic flow. This would allow a crack to pass through a material at a lower stress intensity and cause a smaller reduction in area at fracture. This theory implies that all fractures are essentially ductile and plastic flow occurs in a very small region around the crack tip. Hydrogen is transported to the region around the crack tip by plastic deformation, in this theory, and thus this is a volume effect. Therefore, any similarity between liquid metal and hydrogen embrittlement would be coincidental because they are due to different causes. There is some evidence that hydrogen affects plasticity but this is very difficult to prove because of pressure effects. In fact, the presence of hydrogen may increase or decrease plasticity at the crack tip which has led to theories quite the opposite to Beachem, based on the assumption that hydrogen restricts plastic flow and leads to decohesion at the crack tip. Some of the evidence to support this theory is based on high performance SEM and TEM photomicrographs that suggest, that even in the intergranular cracking mode, the facets of each grain are covered with extremely small, shallow microvoids, resolvable only at magnifications over 5000 X. This may well be the case but it is hard to prove that this evidence of plasticity is the general case and not caused by other effects, such as second phase particles or deformation that occurs after the surfaces have separated. Also, two of the five theories could account for this microplasticity. In any case, a theory that explains hydrogen embrittlement by a volume effect (dissolved hydrogen interacting with dislocations) is at variance with evidence that hydrogen embrittlement is a surface effect in many instances.

3. Decohesion at or Ahead of Crack Tips

This theory is based on the proposed weakening effect that hydrogen has on the cohesive strength of atomic bonds and was developed by Troian[16] and extended by Oriani.[17] It is supposed that the hydrogen accumulates around the crack tip, within a few atomic distances of the crack and lowers the stress required for tensile separation of atoms just ahead of the crack tip. This idea was later modified to account for the plasticity effects (microvoid coalescence) by proposing that the process occurred in two distinct steps. First, decohesion is facilitated by hydrogen in some areas, and, next, the areas not affected by hydrogen are plastically torn. This implies that some areas on every hydrogen embrittled specimen should have some microscopically brittle areas, such as cleavage facets, but this is not the case, for many samples have seemingly 100% microvoid coalescence fractures. There is some debate as to the exact mechanism by which the proposed bond rupture occurs. Some investigators[7] theorize that a crack would propagate in a brittle manner only if the tensile stress at the crack tip became larger than the cleavage stress, before the material could plastically deform by a shear mechanism, to relieve the tensile stress. Therefore, the hydrogen must either decrease the cleavage stress or interfere with the plastic deformation process at the crack tip. Rice[18] proposed that hydrogen inhibited the nucleation of dislocations at the crack tip thus affecting plastic deformation. Decohesion is consistent with the observation that hydrogen embrittlement is a surface effect, but there is doubt as to whether cleavage would occur before plastic deformation. Indeed, if plastic deformation (movement

of dislocations) was made more difficult, then the tensile strength would rise, but this is not the case.

4. Reduction of Surface Energy by Absorption

This theory accounts for hydrogen embrittlement by a reduction in the energy required to create new surfaces by bond rupture.[19] This is a surface effect theory, which is consistent with experimental observations for nickel alloys. This same mechanism can account for liquid metal as well as hydrogen embrittlement. The idea is based on the well known Griffith criterion and for ideal brittle materials. The energy required to rupture bonds (ϕ_b) can be written:

$$\phi_b = 2\gamma_s - \gamma_b \tag{1}$$

where γ_s and γ_b are surface energies of the created surface and removed grain boundary respectively. In the actual case, the total energy required for crack propagation will also include energy used to move dislocations, ϕ_b (creation of the plastic zone):

$$\phi_t = \phi_b + \phi_p \tag{2}$$

Although the plastic energy term will be much greater than the surface energy term, it can be shown[20] that ϕ_p depends on stress in the vicinity of the crack tip, which in turn depends on ϕ_b. In other words, to produce a new crack surface, bonds must be broken. In order to break these bonds, sufficient stresses must be developed at the crack tip, in producing these stresses, a large plastic zone is created. The large plastic zone uses most of the energy needed for this process but the

amount of energy needed to rupture the bonds at the crack tip, although small, controls the size of the plastic zone, and thus the amount of embrittlement. In order to understand how an embrittling agent would lower the amount of energy required to rupture bonds, imagine a crack propagating through a lattice (Figure 1). For crack propagation to occur, bonds of the type $A\text{-}A_o$, $A\text{-}A_1$, would be broken. Such bonds would have potential energy-separation curves shown in Figure 2. To break a bond, stress, σ_m, needs to be exceeded, and this stress is lower when the embrittler atom is present. The reason this stress is lower is that the amount of energy required to break the bond is lower due to chemisorption. The reason the amount of energy required is lowered is that the embrittler atom adds its potential energy to the system when it chemisorbs. This theory can explain many of the effects of hydrogen embrittlement but leaves questions such as why some materials are more susceptible than others and why mercury is a more embrittling environment in some cases and hydrogen in others.

5. Nucleation of Dislocations at Crack Tips

Lynch[7] has proposed that hydrogen assisted cracking is due to the effect of absorption on the nucleation of dislocations at crack tips. He bases his theory on the idea that liquid metal and hydrogen embrittlement produce the same features in many alloys.[21] In liquid metal embrittlement, Lynch argues that chemisorption at the crack tip is the only possible reaction that could account for embrittlement. He reasons that plastic flow at the crack tip is responsible for both liquid metal and hydrogen embrittlement. Much of his case rests on some

Figure 1. A proposed model of crack propagation through a metal lattice in which the embrittler atom interacts with the surface.

Figure 2. Potential energy and stress separation curves for bonds of the type A-Ao with and without chemisorption.

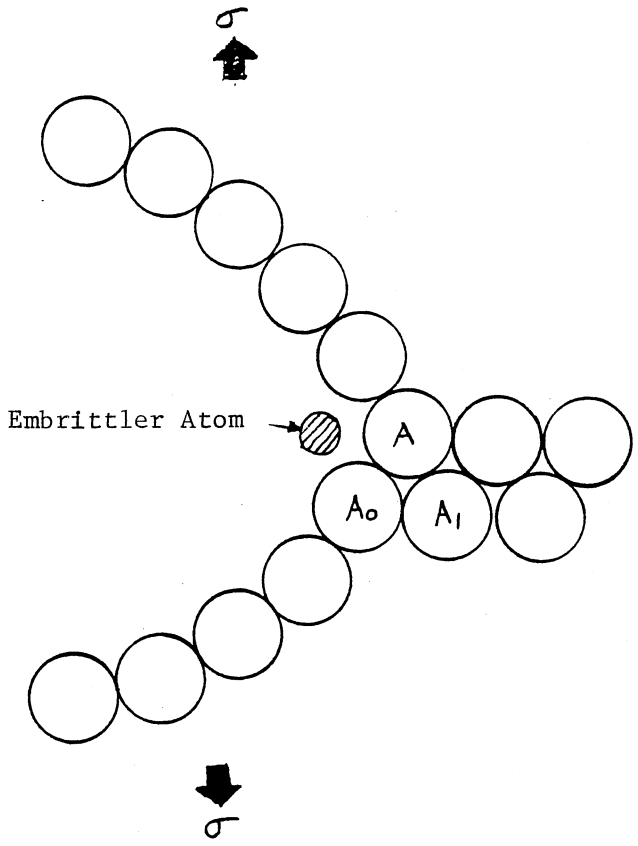
σ
Embrittler Atom
A
A₀
A₁
σ

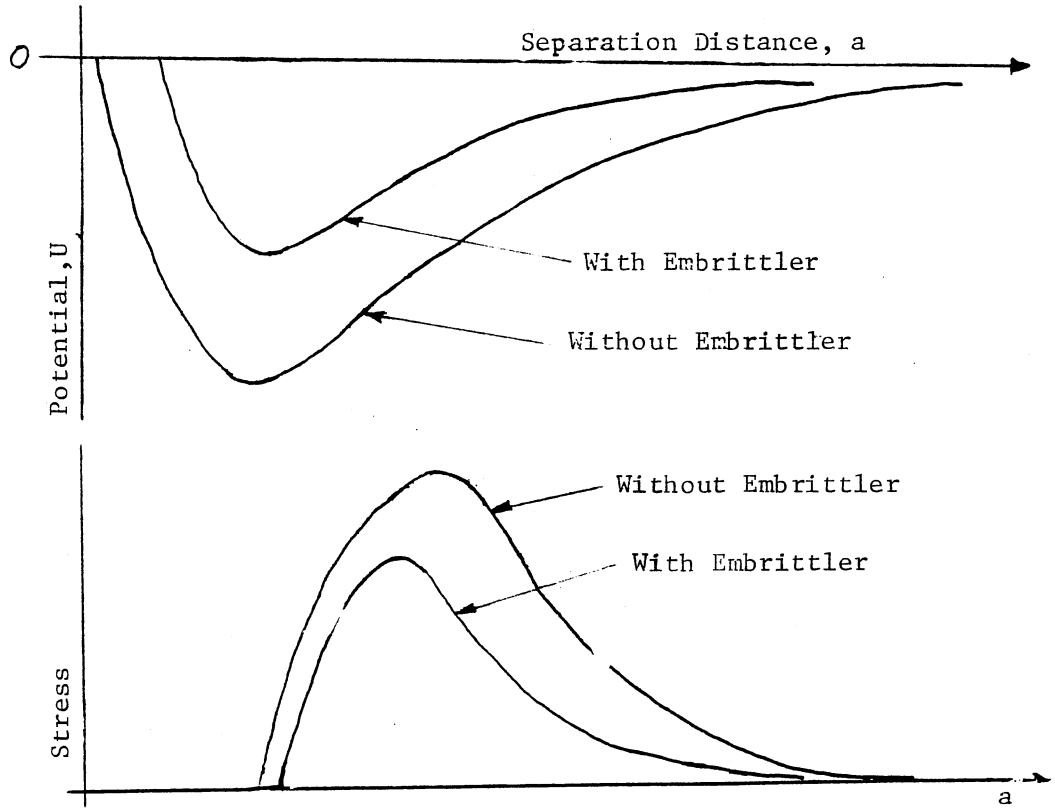
0
Separation Distance, a
Potential, U
With Embrittler
Without Embrittler
Stress
Without Embrittler
With Embrittler
a

experimental work involving ultra high strength steels, that depend on a very fine dispersion of a hard second phase in a ductile matrix to provide strength.[22] Lynch uses high magnification (5000 X) SEM and TEM micrographs to show that even in the intergranular cracking case, grain facets that appear to be flat at lower magnification (500 X) are actually covered with microvoids. He based most of his experimental evidence on materials that would also have a fine, hard, second phase at the grain boundaries. When an intergranular crack occurs, for any reason, these second phase particles would produce some type of pock mark. These pock marks may look similar to ductile microvoids when viewed at very high magnification. These pock marks would not be due to a ductile fracture process but be an artifact of the second phase particles and would occur regardless of the fracture mechanism. To determine if microvoids indeed occur on intergranular fracture surfaces, a material is needed that exhibits intergranular cracking but also has few second phase particles. Such materials include Nickel 200 or Monel 400 that are studied in this thesis. However, Lynch does present a large amount of experimental evidence to show that liquid metal and hydrogen embrittlement produce similar effects in aluminum, nickel, titanium and iron based alloys.[23] Lynch needs to prove three facts to show that his theory could be valid. First, liquid metal and hydrogen embrittlement are the same mechanism. Second, that the mechanism is linked to chemisorption in both cases. Third, the microscopic fracture mode is always ductile. This theory and the reduction of energy theory are very similar and differ only in the exact mechanism by which chemisorption effects the crack tip.

C. Mechanisms of Liquid Metal Embrittlement

Liquid metal atoms are usually about the same size as the atoms in the metal lattice, so interstitial diffusion does not occur, and sub-substitutional diffusion rates are too low to be significant at room temperature. So, liquid metal embrittlement must then be a surface effect because any interaction between a liquid metal and a solid metal must occur at the interface between them.

Liquid metal embrittlement is a simpler process to analyze than hydrogen embrittlement because there are far fewer possible mechanisms. Kamdar[24] has determined that chemisorption is the only possible reaction that could occur during liquid metal embrittlement, at a high enough rate to allow cracks to move at velocities observed during embrittlement. Chemisorption is the reaction of a liquid at the surface layer of atoms in a solid. For this reaction to occur spontaneously a net reduction in total potential energy must result. According to Kamdar, liquid metal embrittlement is due to chemisorption affecting the crack tip in a way that allows the crack to move through the material easier. There are three theories that explain the effect of chemisorbed liquid metal on the crack tip. These theories are almost the same as the last three theories presented already to explain hydrogen embrittlement. They are the decohesion at the crack tip, reduction in surface energy due to absorption, and the nucleation of dislocations at the crack tip. The theories differ with their counterparts that are proposed to explain hydrogen embrittlement only in that mercury is chemiabsorbed instead of hydrogen. Each theory still retains the

relative strengths and weaknesses outlined eariler.

D. Observations Concerning Liquid Metal and Hydrogen Embrittlement

The literature contains much information concerning the effects of hydrogen on steel. Less information is available concerning liquid metal and hydrogen embrittlement of nickel and its alloys. This information can be divided into two catagories, generally accepted observations and controversial observations.

1. Generally Accepted Observations

Some observations are common to the works of many authors and are the cause of little or no disagreement. These are presented below. It has been shown the hydrogen and mercury embrittlement do not significantly affect the tensile strength of any nickel alloy under any condition.[5,23] Even in the most severe case, the embrittlement of Monel, which is intergranular, the tensile strength was only slightly reduced.[5,19] One investigator[25] has reported a reduction in tensile strength in ultra pure Inconel 600.[25] However, these tests were performed on very fine wires (0.8 mm) which means a large surface to volume ratio and a domination of surface effects. Another commonly observed feature is that hydrogen embrittlement and liquid metal embrittlement cracks begin on the surface and grow inward during a slow tension test. This leads to a fracture much different in macroscopic appearance than the normal cup and cone fracture where the cracks start on the inside and grow outward.[26,27] Additionally, it has been shown[27] that no cracks are nucleated until significant amounts of strain have

occurred and different materials require different amounts of strain to nucleate surface cracks. The only exception to the rule is fractures that exhibit almost 100% microvoid coalescence and these fractures are accompanied by small losses in ductility. The affect of embrittler concentration upon the extent of embrittlement is another area where it is agreed that increased embrittler concentration leads to increased embrittlement effects. In liquid metal embrittlement, this effect has been shown by Kamdar[28] for the embrittlement of Cadmium by Indium, using mercury as an inert carrier (Figure 3). In hydrogen embrittlement, it has been shown, for Monel alloys, that changing current, hence embrittler concentration affects the extent of embrittlement[19] (Figure 4). Common to all studies are the fractographic features found in both the hydrogen and mercury embrittled specimens. The general sequence of features is intergranular, transgranular and then microvoid coalescence. Each stage may be accompanied by secondary cracking and not every stage occurs on every fracture. In mercury or hydrogen assisted fatigue fractures, the same cracking modes and orders are observed.[7] In both the hydrogen and mercury assisted fatigue, the fatigue crack propagation rates were increased.[13] Data from Lynch[23] show increases in the fatigue crack growth rate, as measured by striation spacing, in nickel single crystals by a factor of five in both environments. Data from Price and Good[29] show a reduction in fatigue life in 10 different nickel alloys in mercury. There are also data[13] to show that, in Inconel 600, lowering the frequency of testing increases the crack growth rate. Also, this same study shows that hydrogen precharging and mean stress have little to no affect on the crack growth rate. In mercury, these kinds of data are not in the literature. In the slow strain rate

Figure 3. Variation in ductility of polycrystalline cadmium with the indium content of a mercury-indium surface coating.

Figure 4. Variation of ductility with hydrogen charging rate for Monel 400.

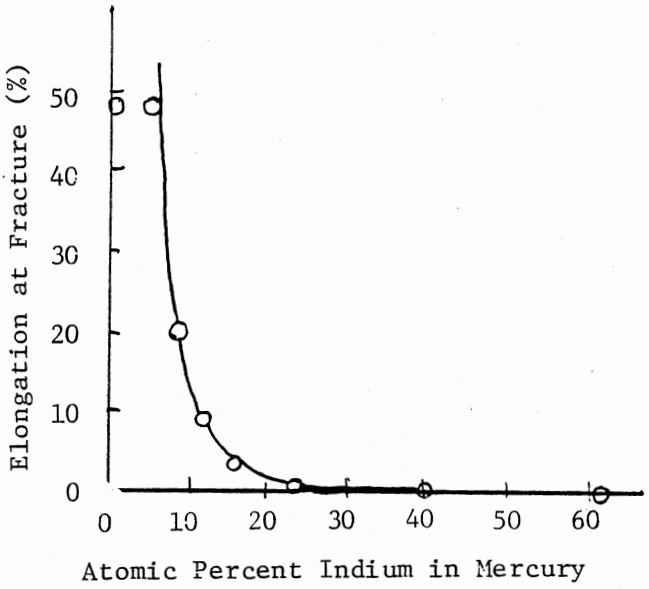
Elongation at Fracture (%)
50
40
30
20
10
0
0
10
20
30
40
50
60
Atomic Percent Indium in Mercury

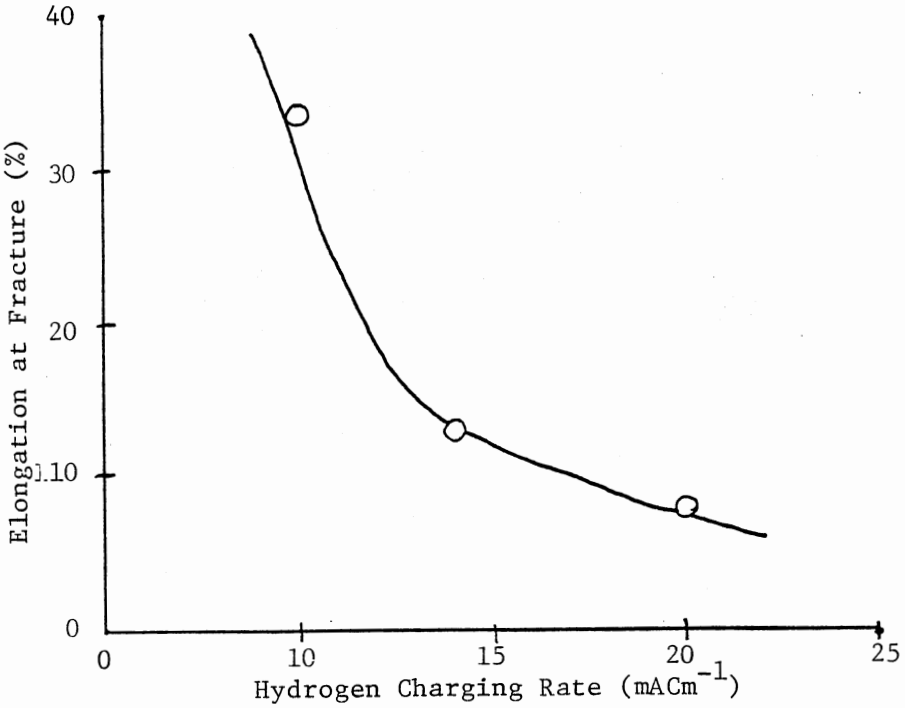
Elongation at Fracture (%)
40
30
20
10
0
0
10
15
20
25
Hydrogen Charging Rate (mACm^{-1})

tensile tests, it has been shown that lower strain rates cause more embrittlement affects. This is true for all alloys tested and in both the mercury and the hydrogen environment.[30] Both electrolytic and gaseous hydrogen produce similar features on the same alloys, so it appears that the source of hydrogen does not influence the type of embrittlement. As far as the electrolytic charging solution is concerned, it has been shown[31,32] that the hydrogen, not the charging solution, causes the embrittlement in nickel based alloys and the only effect of changing the solution is to change the hydrogen entry rate. Lynch[23] has discovered that in mercury and hydrogen embrittlement and even stress corrosion cracking of many FCC alloys including nickel, in single crystals, the crack path was always parallel to the {100} plane and crack growth direction was <110>.

2. Controversial Observations

Several investigators, including Lynch, have theorized that hydrogen and liquid metal embrittlement are the same mechanism. The similarities are very apparent from the large amount of fractographic evidence gathered from several different materials by Lynch.[23] However, many theories of hydrogen embrittlement cannot accomodate this idea because they are based on a volume effect. Although a large body of experimental evidence supporting these theories has been gathered, no evidence has been presented to date that proves the liquid metal and hydrogen embrittlement do not have the same mechanism. Another issue is the effect of stacking fault energy on hydrogen embrittlement of nickel alloys. Some researchers[15] have argued that the more planar the slip, the more the embrittlement. Experiments have been done on stainless

steels[33] and nickel based alloys[34] to show this correlation. The experiments are based on the idea that decreasing the stacking fault energy promotes planar slip, alloying elements, such as Chromium and Molybdenum, lower the stacking fault energy[35] and therefore highly alloyed nickel alloys would be more susceptible to hydrogen embrittlement than lower alloy materials, under this theory. The basis of this idea is that hydrogen diffusion is increased when planar slip occurs. Thompson[34] has proposed planar slip promotes increased embrittlement and this increased embrittlement can be correlated to a decrease in average void size. He reasons that if hydrogen transport was increased, then hydrogen assisted void nucleation would increase. If more voids are nucleated, then the average void size would be smaller, therefore, the amount of embrittlement can be correlated to the average decrease in void size, for a given material, which can be correlated to the planar slip and finally to the amount of alloying elements. This is relatively recent work and further evidence is not available.

The final and most controversial observations are the affect of impurities on the extent and type of embrittlement. The elements phosphorus, sulfer, tin, and boron have an effect on the embrittlement of nickel alloys according to some researchers. However, the cause, amount and even the type of effects are a center of much disagreement. Most of the experimental work is generally done the same way. A material, with some chosen impurity, is tested in the furnace cooled and the quenched state. The furnace cooled sample would presumably have this impurity at the grain boundaries, while the quenched sample would not. The samples were fractured in the environment selected, and the two sample states are compared for the degree of embrittlement, especially with

respect to the amount of intergranular embrittlement. Next, an Auger spectrum analysis was performed on the intergranular fracture surface to determine the composition of the surface layer (an Auger spectrum is an electron energy surface analysis technique). The chosen element was segregated at the grain boundaries and caused an increased or decreased embrittlement. The most studied element is phosphorus. Funkenbusch[19] stated that in Monel 400 the segregation of phosphorus to the grain boundary causes decreased embrittlement, as measured by elongation at fracture. He attributed this effect to either the improvement of grain boundary cohesion or to increase grain boundary packing efficiency. He noticed the same effect in both the mercury and hydrogen embrittled specimens. He discounted the affect of phosphorus on grain boundary cohesion due to other studies that show that cohesion is decreased by the presence of phosphorus. Another study,[30] involving the nickel based alloy Hastelloy C-276 in hydrogen, shows that embrittlement (as measured by time to fracture) was increased by phosphorus segregation. It showed that embrittlement occurs in two distinct stages as a function of aging time. The first stage, which occurs relatively quickly, is attributed to short range ordering, while the second stage, which occurs after some time, is attributed to long range ordering. It is proposed that ordering causes more planar slip, and planar slip causes increased hydrogen transport, thus increased embrittlement. These two studies are just examples of the research in this area. Clearly, the exact effect of phosphorus segregation is still not known. The effects of other elements that are known hydrogen recombination poisons has also been researched. Latanison[32] has proposed that, in nickel 270, the segregation of tin to the grain boundaries acts to increase hydrogen absorption into the

material, because tin acts as a hydrogen recombination poison. Other elements such as boron and sulfer have also been similarily studied. The conclusions that can be drawn from this experimental evidence are that the results are not consistent from one investigator to the next, and that theories based totally on this type of experimental evidence may be hazardous. It is interesting that aging affects the amount of hydrogen embrittlement in such a way, and there may be some unforeseen variable affecting the testing. Cornet[25] has attempted to eliminate any unforeseen impurity by using ultra pure materials to examine the affect of carbon, phosphorus and tin on the embrittlement of Inconel 600. The maximum level of impurity in his samples was 20 parts per million and great pains are taken to prevent contamination. Each sample to be tested was doped with the element to be examined, and the sample was tested in the usual way. His conclusions are that impurity segregation had no effect on the amount of hydrogen embrittlement for the impurities tested.

CHAPTER III

EXPERIMENTAL

A. Introduction

The testing was limited to slow strain rate (SSR) tensile tests and pulsating tension fatigue tests, using the materials testing system (MTS machine). The test specimens were the same for both the tensile and fatigue tests, and were similar to rotating beam fatigue specimens, with dimensions given in Figure 5. A 600 grit surface was used initially and for fatigue tests, but an as machined surface proved to be satisfactory for tensile tests. In the surface cracking studies, the sample surface was chemically polished in a solution of mixed acids.[36] To obtain a known current density, a known area was exposed to the solution by isolating all but the center 12.5 mm of the sample by tape. In the mercury testing, the technique of Price and Good[5] was used.

In the hydrogen testing, unless otherwise specified, the following conditions were used. The charging rate was 400 Am^{-2}, the sample was precharged 2 hours before the test, and charging continued during testing. Displacement control was used on the MTS machine with a ramp velocity of 7.6×10^{-4} mmS^{-1}. The testing was done at room temperature. The following technique was generally used for these tests. First, the sample diameter was measured and recorded, then the sample gage length was isolated by tape. The sample was then placed in the cell, the appropriate solution was poured in and the potentiostat connected.

Figure 5. Test specimen configuration.

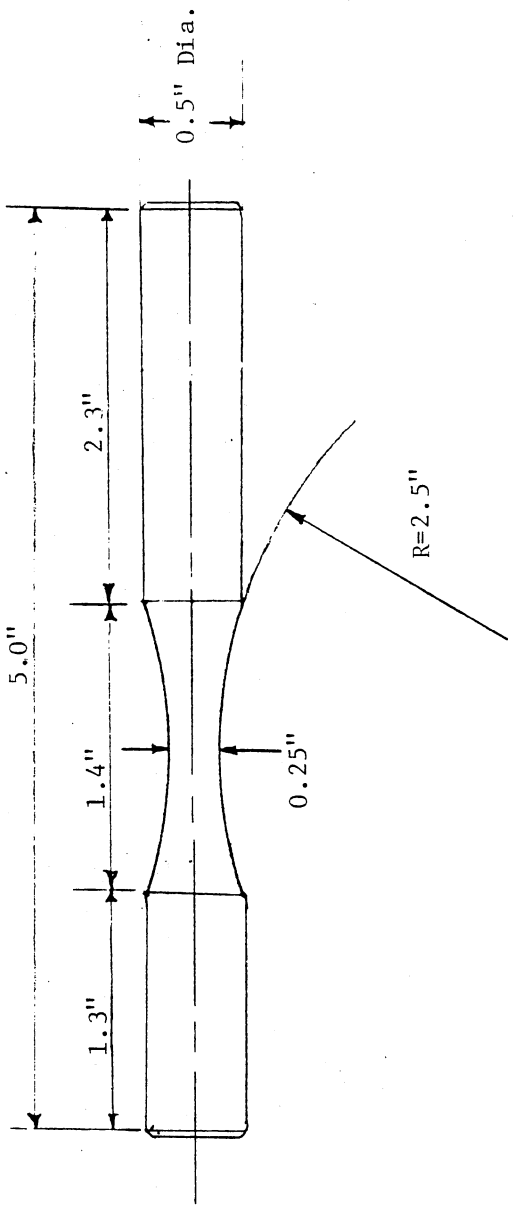
0.5" Dia.
2.3"
5.0"
1.4"
1.3"
0.25"
R=2.5"

The sample was then placed into the testing machine grips. If this were a slow strain rate (SSR) tensile test, the appropriate rate was selected on the function generator. This function generator controls the rate (velocity) at which the grips separate. During testing, usually the current was maintained thus hydrogen charging continued throughout the test. Slow strain rate tests took 3-4 hours typically, depending on the sample ductility. If a fatigue test were being performed, the same sample preparation procedure was followed. After the sample was placed in the machine, a sine wave was generated by a function generator, and this wave was converted into force and applied to the specimen. The stress varied sinusoidally between 0 and 75% of the tensile strength typically. The frequency used was a variable over the range of 3 to 40 Hz, but was constant during a test. After a sample failed, it was cleaned in the ultrasonic cleaner, first in water, then in an organic solvent. The fracture surface was then examined in the stereo zoom microscope (SZM) and in the scanning electron microscope (SEM). The reduction in area was measured using a caliper type micrometer, on the smallest cross section in the necked region.

B. Equipment Used

The materials testing system (MTS) can be described as an electro-mechanical, feedback controlled testing system. The controlled variable can be either load, stroke (position) or strain. An electrical voltage, corresponding to one of these three variables is fed into the hydraulic control unit. This unit also receives feedback signals from a load cell, a LVDT and a strain gage. The appropriate feedback signal is compared to the input signal and an error function is generated. This error

signal drives the hydraulic servovalve in the proper direction to eliminate the error. The load, strain or stroke is read directly from the feedback sensors and is displayed on the digital indicator. This indicator also stores the largest load encountered, which is used when calculating the tensile strength. The system has a capacity of 55,000 pounds and a resolution, when used in the configuration needed for this testing of $\pm$.0005 in and $\pm$5 pounds.[37] The system uses self tightening grips to hold the specimen. The hydrogen is generated electrolytically. The amount of hydrogen generated depends on the current density. The current, in this study, was controlled using a Princeton Applied Research model 173 Galvanostat, to within 0.2% of the scale reading.[38] The specimen was the cathode with a platinum wire anode. In this way, the hydrogen was generated at the specimen surface. The cell used for the hydrogen testing was made of plexiglass and steel, with all steel parts coated with paraffin (Figure 6a). The mercury testing cell was made of steel and was coated with epoxy (Figure 6b). The electron microscope used was a Jeol model 35. The mercury used in this study was triple distilled instrument grade. The solution, used as an electrolyte in the hydrogen embrittlement tests, consisted of distilled water with sulfuric acid (H_2SO_4) added to give a pH of 3.2, plus 0.25 gl^{-1} of sodium arsenate as a hydrogen recombination poison. This solution is recommended by ASTM for moderate charging rates.[31] All chemicals used were reagent grade.

C. Experimental Technique

The samples were machined out of round bar stock, 12.5 mm diameter. The bar stock was cold drawn and the specimens were machined along the

a. Cell used for hydrogen testing.

b. Cell used for mercury testing.

Figure 6. Environmental test cells used in this study.

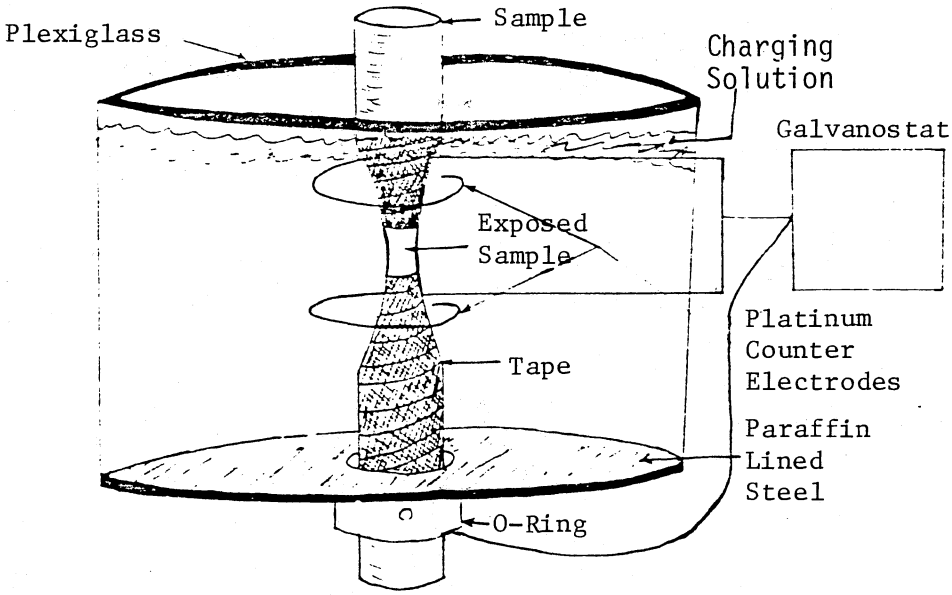
Plexiglass
Sample
Charging
Solution
Galvanostat
Exposed
Sample
Tape
Platinum
Counter
Electrodes
Paraffin
Lined
Steel
O-Ring

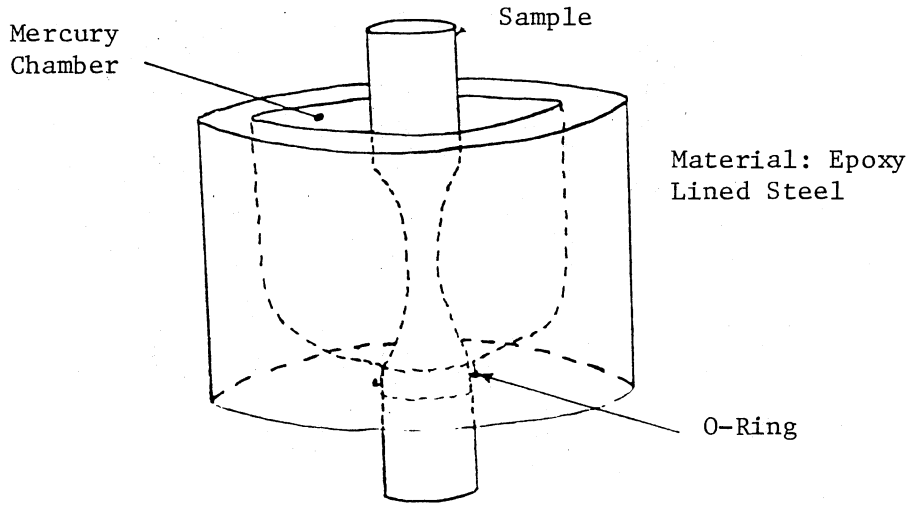
Mercury
Chamber
Sample
Material: Epoxy
Lined Steel
O-Ring

cold working direction. The as machined surface was polished to a 600 grit surface finish when needed. The annealed specimens were heat treated in a furnace under a mild vacuum (about 25 Pa) for 1 hour at 750 C typically. After they were taken out of the furnace, all scale was removed by sanding. For the void size and distribution measurements, the following technique was used. Photographs were taken of typical microvoid areas in the SEM at 500 magnification. The specimen was always aligned with the viewing plane to assure accurate magnification; next, a transparent overlay, with 5 μm and 10 μm equivalent size circles was placed on the photograph. The voids on the photograph were sorted and counted according to the overlay.

CHAPTER IV

RESULTS AND DISCUSSION

A. Results

1. Tests in Mercury

The tests of Price and Good[5,29] were not repeated, but their fractured specimens were studied and additional measurements made. Further testing was done when necessary. The alloys studied are given in Table I and, the results in Table II. The tests used by Price and Good were similar to the SSR tensile and fatigue tests used in the present study. The results show that all alloys could be embrittled to some extent by mercury, as determined by a reduced reduction in area, yet the tensile strength was not significantly reduced in any alloy in mercury. A cup and cone fracture with cracks beginning in the interior, which was the normal mode for these SSR tensile tests, was replaced by a flat or slant fracture with cracks growing from the outside inward, in all but Incoloy 800 and Incoloy 825. Examples of fractures in mercury are shown in Figure 7. The Incoloys were least embrittled, showing an essentially microvoid type fracture surface and little change in reduction of area over samples tested in air (Figure 8). Monel 400 was the most embrittled alloy, having a 100% intergranular fracture surface, while Monel R405 was embrittled to a much lesser extent, the fracture surface starting out intergranular but a transition to transgranular and then

TABLE I

ALLOYS TESTED BY PRICE
AND GOOD

Alloy	Hardness R_B	Yield Str. MPa	Tensile Str. MPa	Fatigue Stress MPa
N02200	53	105 15,2	554	500
N02200*	88	880 127.6	750	710
N04400	70	280 40.6	581	420
N04400*	98	770 111.6	935	700
N04405	72	245 35.5	672	420
N04405*	98	791 114.7	966	770
N05500	84	560 81.2	630 - loades low	504
N06600	81	357	826	560
N06625	100	609	940	700
N07718	95	637	924	672
N07750	31 (R_c)	826	1218	1008
N08800	83	329	756	560
N08825	87	511	784	560

*Cold Worked

TABLE II

RESULTS OF PRICE AND GOOD

Alloy	Reduction in Area (%)		Fatigue Life (10^3 cycles)		Tensile Strength (MPa)	
	Mercury	Air	Mercury	Air	Mercury	Air
N02200	60	84	49	200	548	554
N02200*	59	73	130	265	840	861
N04400	11	67	3.4	630	579	581
N04400*	4	54	52	200	892	935
N04405	20	62	7	241	672	672
N04405*	12	54	28	47	963	966
N05500	9	74	12	360	582	630
N06600	12	65	60	200	754	826
N06625	6	63	170	400	940	940
N07718	12	58	74	190	920	924
N07750	13	35	44	62	1198	1218
N08800	39	65	22	490	687	756
N08825	68	66	28	170	785	784

*Cold Worked

a. A typical cup and cone fracture of Incoloy 800 tested in mercury.

b. A typical slant fracture. Monel R405 tested in mercury.

Figure 7. The two types of fractures that occur in the mercury environment for the SSR tensile test.

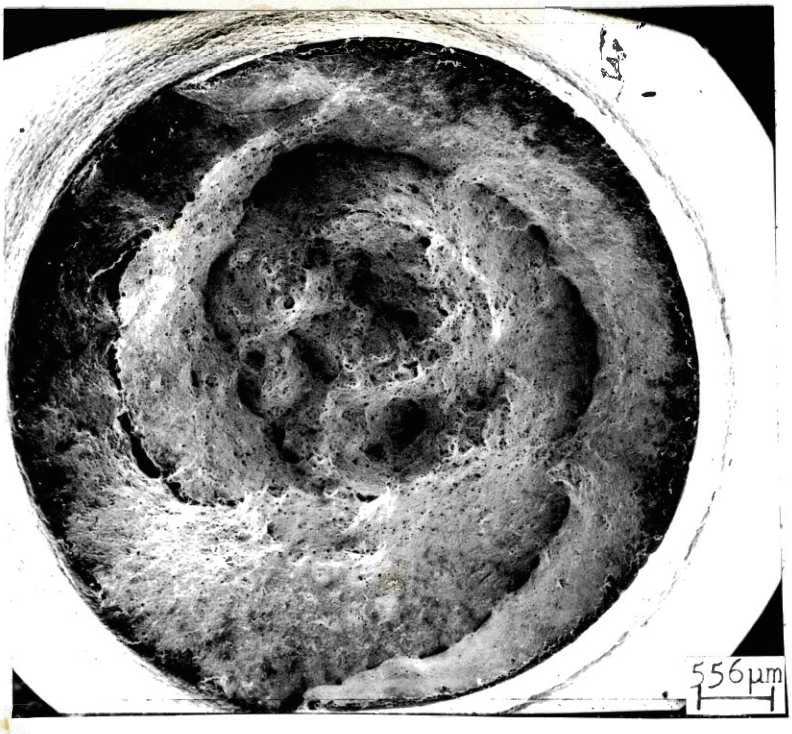
556µm

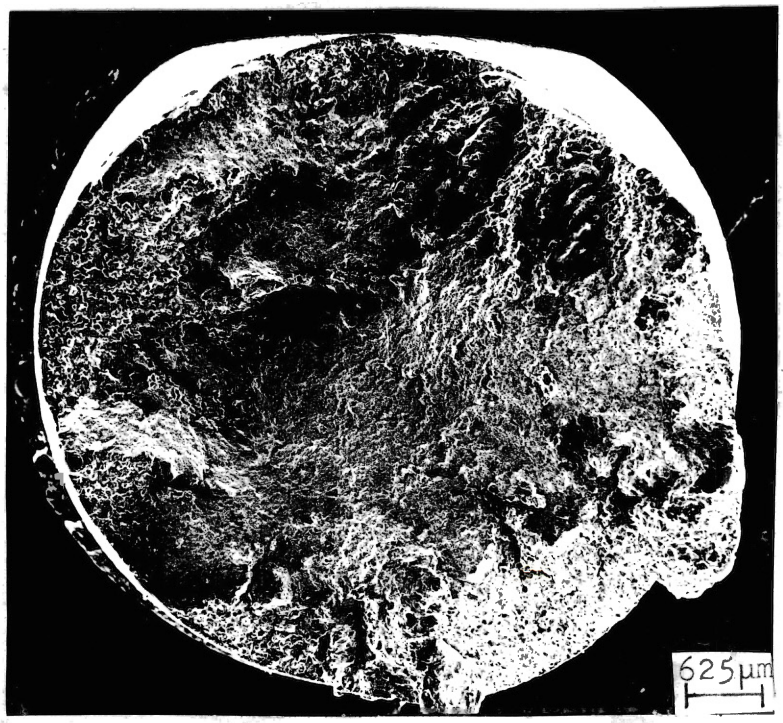
625µm

microvoid coalescence occurred (Figure 9). Nickel 200 showed intermediate behavior, with a wide variety of fracture surface features as shown in Figure 10. Inconel 600 behaved similarly to Nickel 200, while Inconel 625 behaved like Monel 400. In the alloys that showed some necking, extensive side cracking occurred, which was either 45° to the stress axis and transgranular, or 90° to the stress axis and intergranular. The strain rate and the amount of cold work affected the extent of embrittlement. If the strain rate were lowered, more embrittlement would occur and the side cracking would change modes from 45° to 90° to the stress axis (Figure 11) and side cracks became less numerous. Cold working led to less embrittlement and a tendency toward transgranular rather than intergranular fracture modes. The fatigue tests in mercury led to reduced lifetimes for all alloys (Table II). Fractographic features were similar to the SSR tensile test but striations, normally associated with fatigue were only occasionally seen. They were not seen in Monel 400. The fatigue test seemed to cause more embrittlement than the SSR tensile test, because intergranular fatigue zones formed on Inconel 800 and Inconel 825, both of which were not severely affected by the SSR tensile test in mercury.

2. Exploratory Tensile Tests in Hydrogen

In light of the similarities for the different alloys in mercury, not all of the same alloys were tested in hydrogen, rather representive alloys for each category were chosen, Nickel 200, Monel 400, Monel R405, Inconel 625, Hastelloy C-276 and Incoloy 825. The results, Table III, showed no drop in the tensile strength occurred between the hydrogen and air environments but a reduced reduction in area did occur in most

Figure 8. A Monel 400 fractured in air. This is a cup and cone fracture, which is the normal mode for SSR tensile tests in air.

a. The fracture surface of a Monel 400 tested in mercury. This mixture of intergranular and transgranular crystallographic fracture modes was almost constant across the surface.

Figure 9. Fractographic features found in Monel in Mercury.


25μm

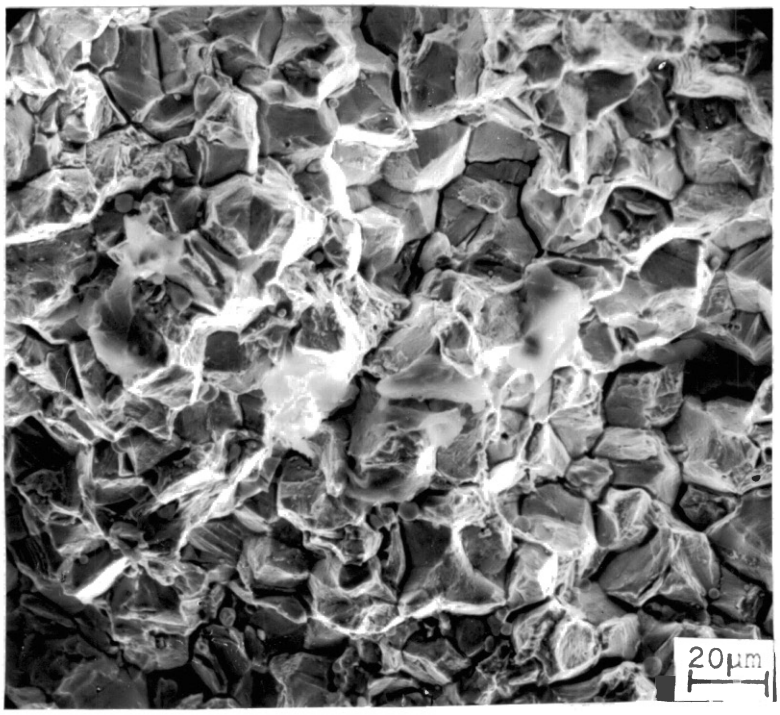
20μm

b. A Monel R405 fracture surface under conditions identical to Figure 9a. The fracture began similarly to Monel 400 but a change to a transgranular mode with tearing and maybe microvoids occurred toward the midsection, as shown.

Figure 9. Continued

a. A transgranular crystallographic fracture surface of Nickel 200 tested in mercury. This is a typical fracture surface in the area toward the outside edge of the specimen.

Figure 10. Fractographic features found in Nickel 200 in mercury.

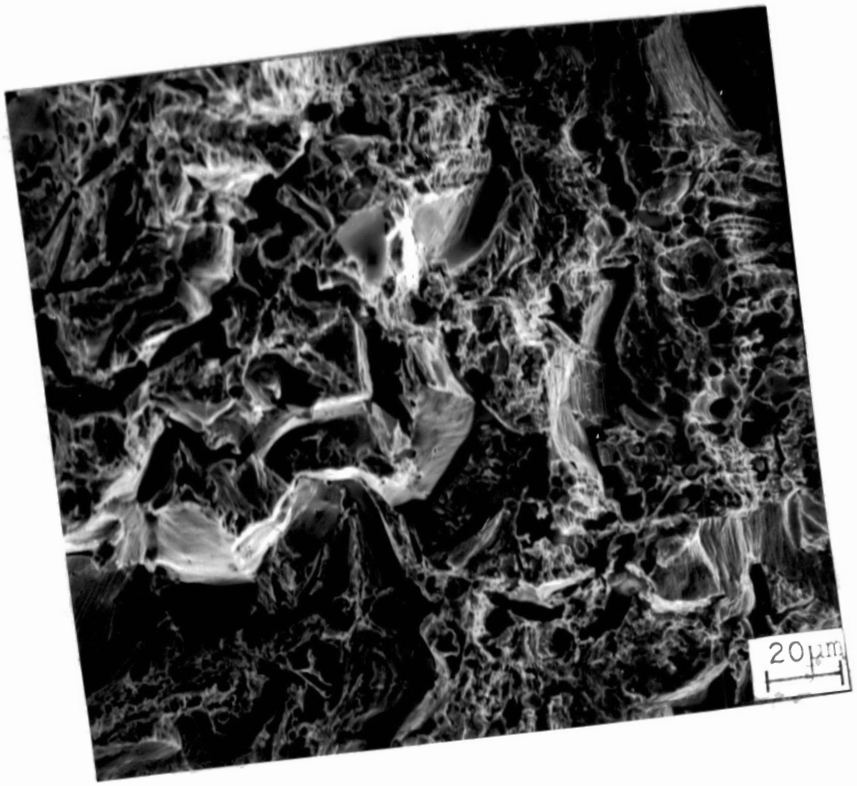
20μm

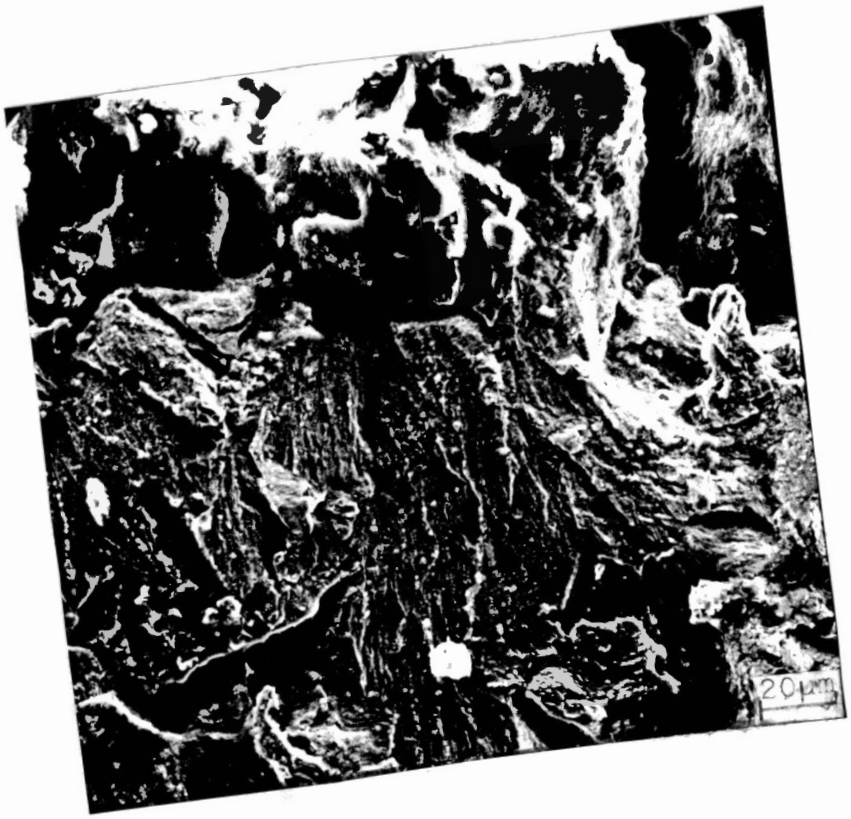
20μm

b. A bit further in the fracture mode changes to non-crystallographic transgranular with no secondary cracking.

c. Toward the center of the Nickel 200 specimen, the fracture changes to microvoid coalescence.

Figure 10. Continued.

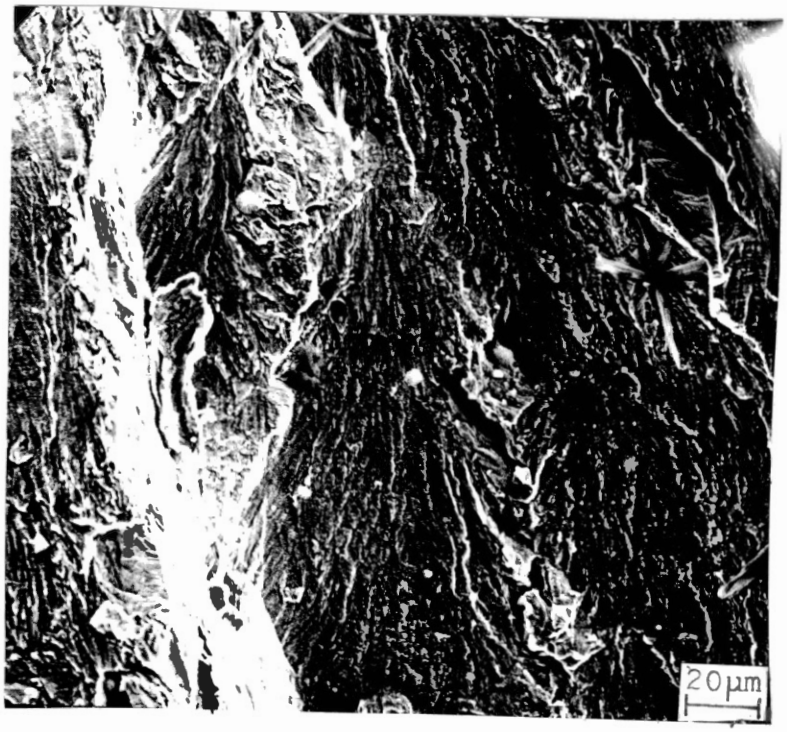
20μm

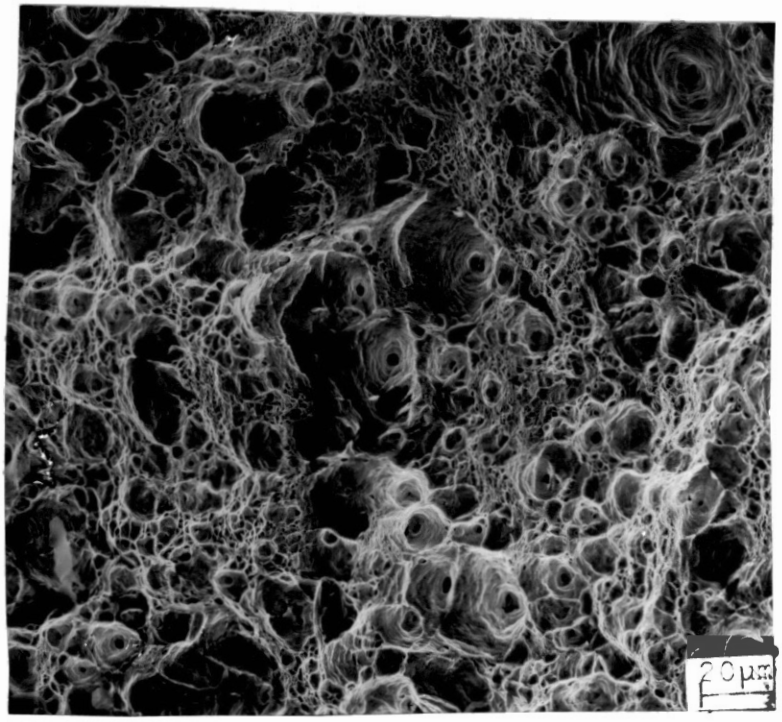
20μm

a. 45° to the stress axis cracks that occur in the necked region of a SSR tensile test of Nickel 200.

b. 90° to the stress axis cracks that occur in the necked region of a SSR tensile test of Monel 405.

Figure 11. Side cracking found in mercury.

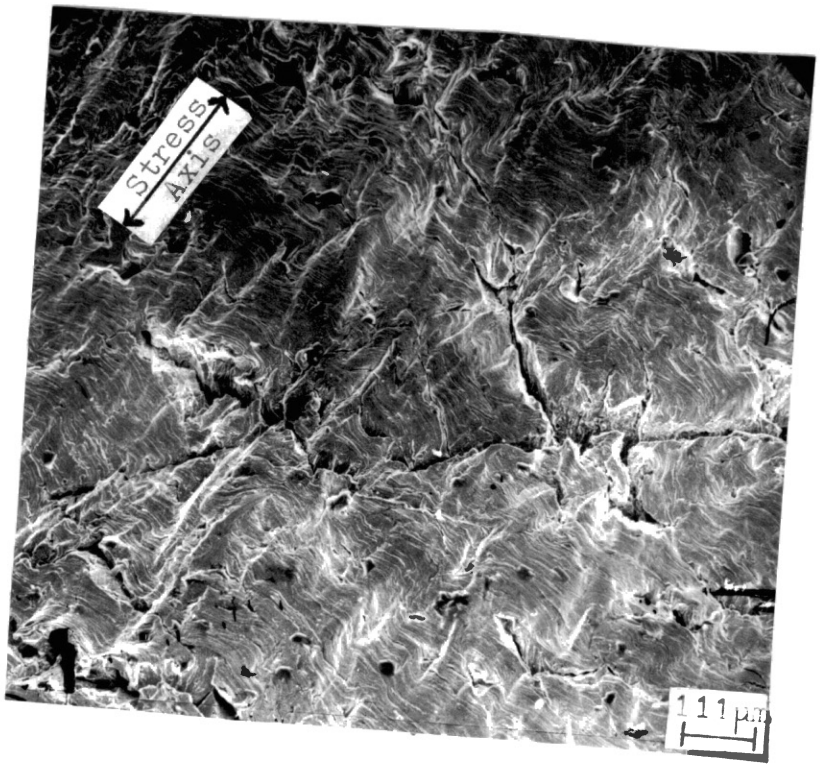
Stress
Axis
111 μm

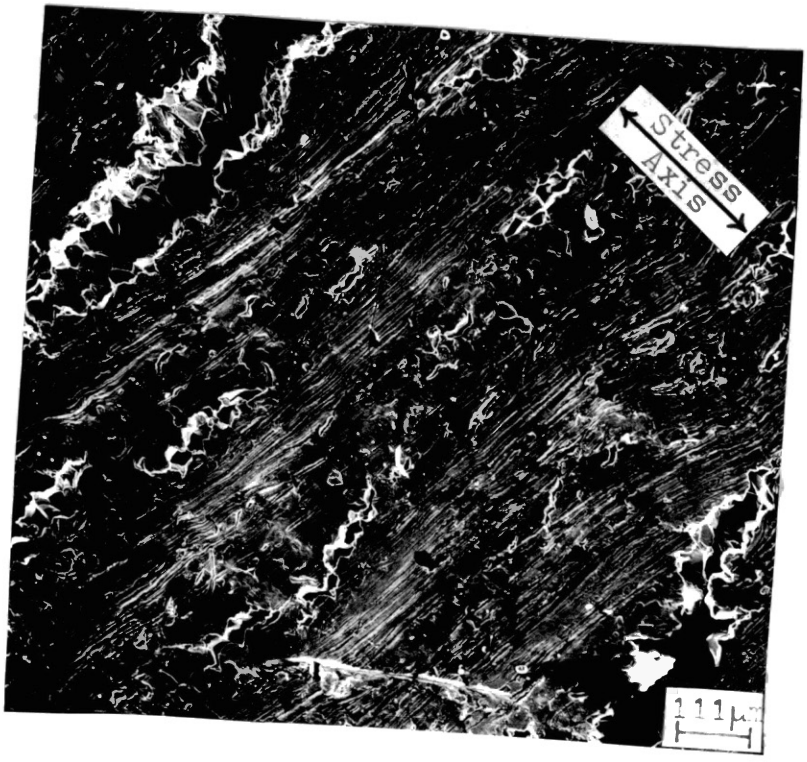
Stress
Axis
111 μm

TABLE III

HYDROGEN EMBRITTLEMENT DATA

Alloy	Reduction in Area (%)		Tensile Strength (MPa)	
	Hydrogen	Air	Hydrogen	Air
N02200	39	84	526 (76.2 ksi)	536
N02200*	38	73	871	880
N04400	12	67	570	581
N04400*	14	54	881	935
N04405	30	62	616	672
N06625	39	63	990	940
N06625*	33	41	1636	1654
N10276*	56	67	860	890
N08825	67	68	760	784

*Cold Worked

alloys. The fracture mode changed from an internally initiated, cup and cone fracture in air to a surface initiated flat or slant fracture in hydrogen (Figure 12). The exception was Inconel 825 which had a cup and cone fracture in hydrogen. Side cracking occurred in every alloy. Cold work caused less embrittlement in all alloys, as evidenced by less intergranular cracking and an earlier onset of microvoid type fracture surfaces. Below are some observations for each class of alloy.

Nickel. Nickel was the base material for all alloys tested and showed the widest range of features. The degree of embrittlement was moderate, somewhere between the Monel and Inconel 625. The wide range of features, from transgranular crystalographic to microvoid coalescence are shown in Figure 13.

Nickel-Copper Alloys. Monel 400 gave the most embrittlement of any alloy in hydrogen. The fracture surface was essentially homogeneous with a mixture of intergranular and transgranular crystallographic modes as shown in Figure 14. Monel R405 gave much less embrittlement. Monel R405 fractures in hydrogen started intergranular, like Monel 400, but a transition to transgranular then to microvoid coalesence occurred. A large amount of secondary cracking accompanied the transgranular region (Figure 15).

Nickel Chromium Alloys. Alloys Hastelloy C-276 and Inconel 625 behaved similarly when tested in hydrogen. Both alloys had a small rim of mixed crystallographic and non-crystallographic fracture surface (Figure 16) which led, within a millimeter, to a microvoid type fracture surface. The fracture started from the outside and both cases showed extensive side cracking.

a. A typical cup and cone type fracture of Incoloy 825 in hydrogen. Notice the similarity to Figure 8.

b. A typical SSR tensile test fracture in hydrogen. The failure started from the outside surface. The material is Inconel 625.

Figure 12. The two failure modes found in the hydrogen environment for SSR tensile tests.

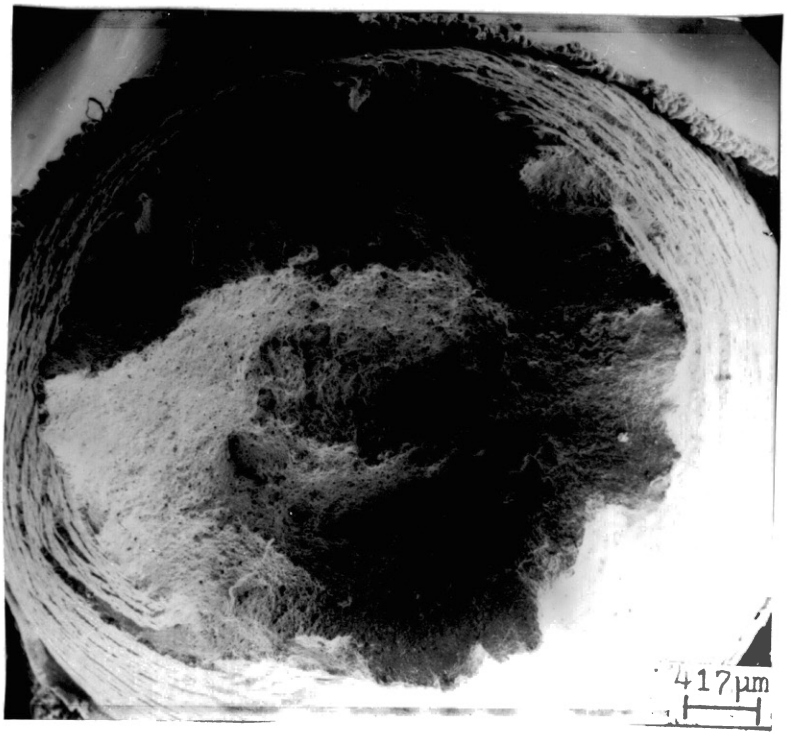
417µm

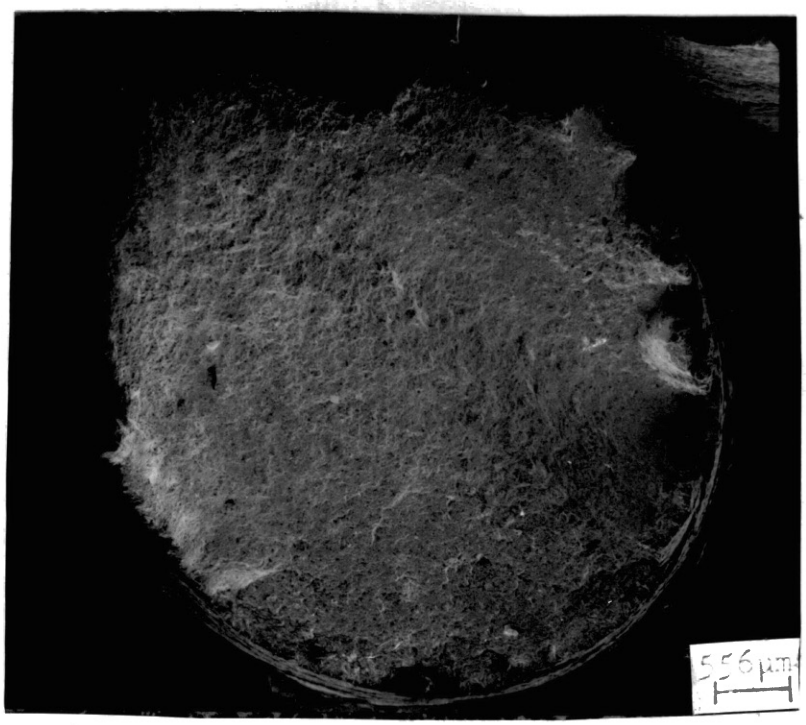
556µm

a. A Nickel 200 fracture surface toward the outside edge. This crystallographic transgranular mode is typical of the edge area.

b. A Nickel 200 fracture, a bit in from the edge where the fracture mode changes to transgranular crystallographic and non-crystallographic with secondary cracking.

Figure 13. Features found in Nickel 200 fractured in hydrogen.

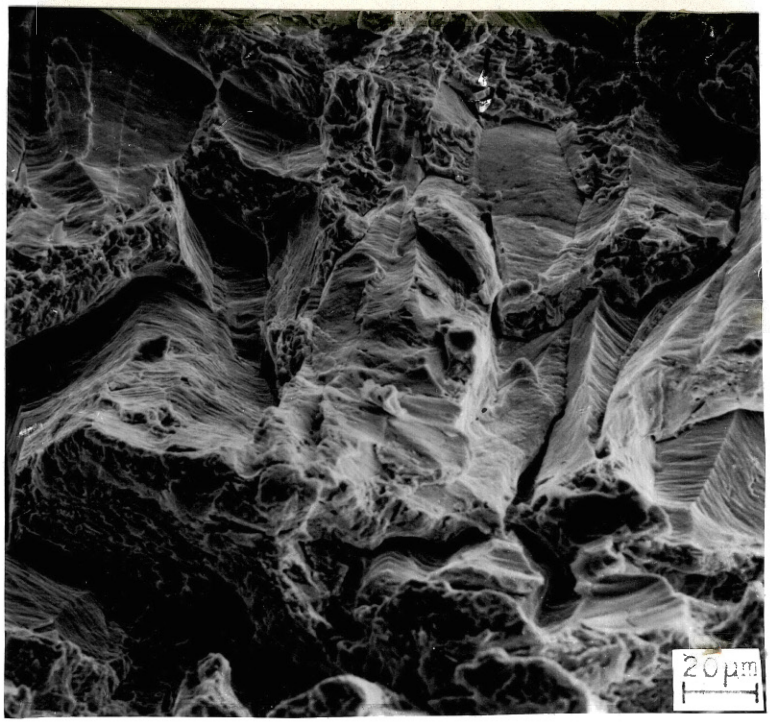
20μm


20μm

c. A Nickel 200 specimen, between the edge and the center where non-crystallographic transgranular with no secondary cracking is present.

d. Toward the center of this Nickel 200 specimen the fracture mode goes to microvoids.

Figure 13. Continued.

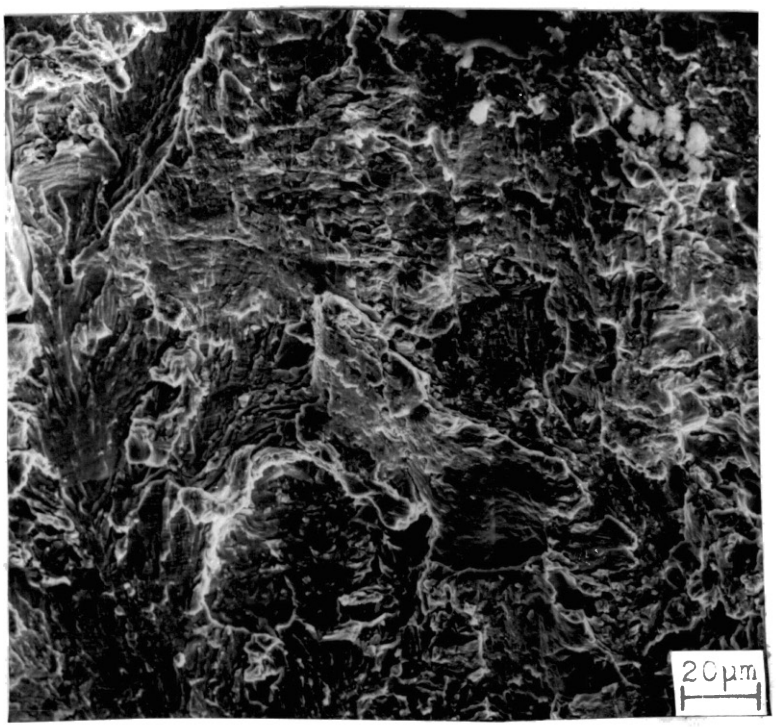
20μm

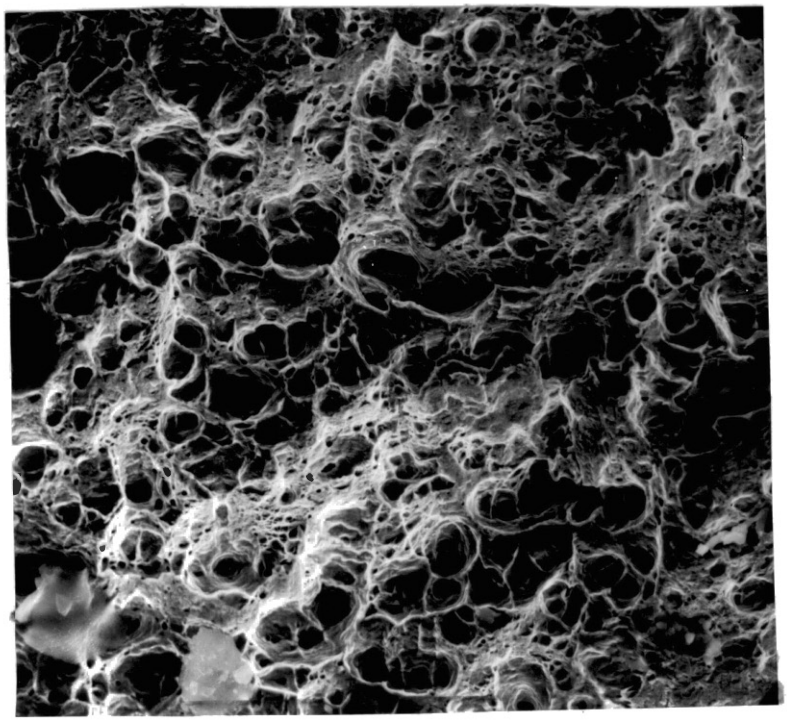

Figure 14. The fracture surface of Monel 400 tested in hydrogen. The fracture mode was mostly intergranular with some transgranular tearing.

Figure 15. The fracture surface of Monel R405 looked the same as Monel 400 at the outside edge but a change to transgranular crystallographic with secondary cracking (as shown in this figure) and then to microvoid coalescence occurred toward the center of the specimen.

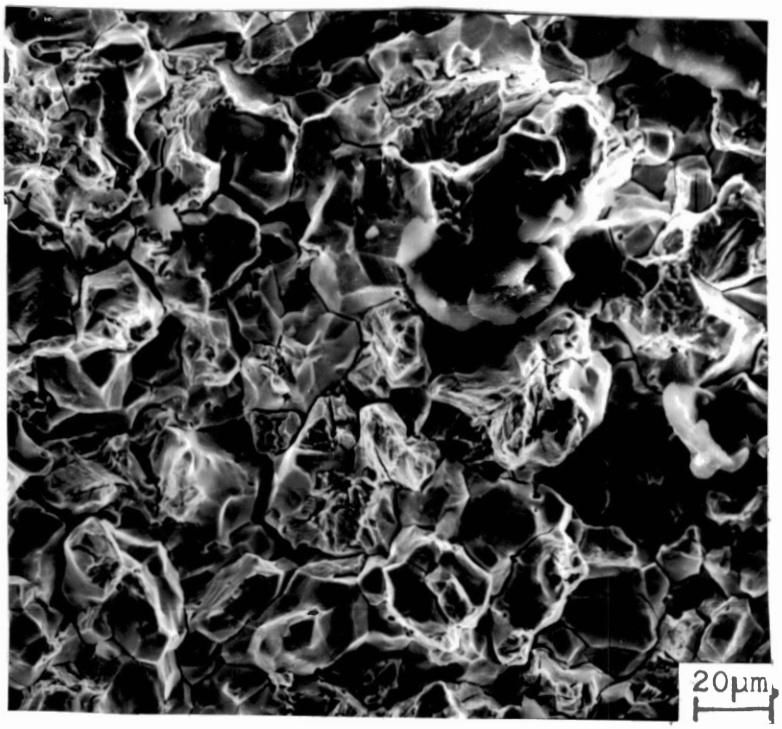
20μm

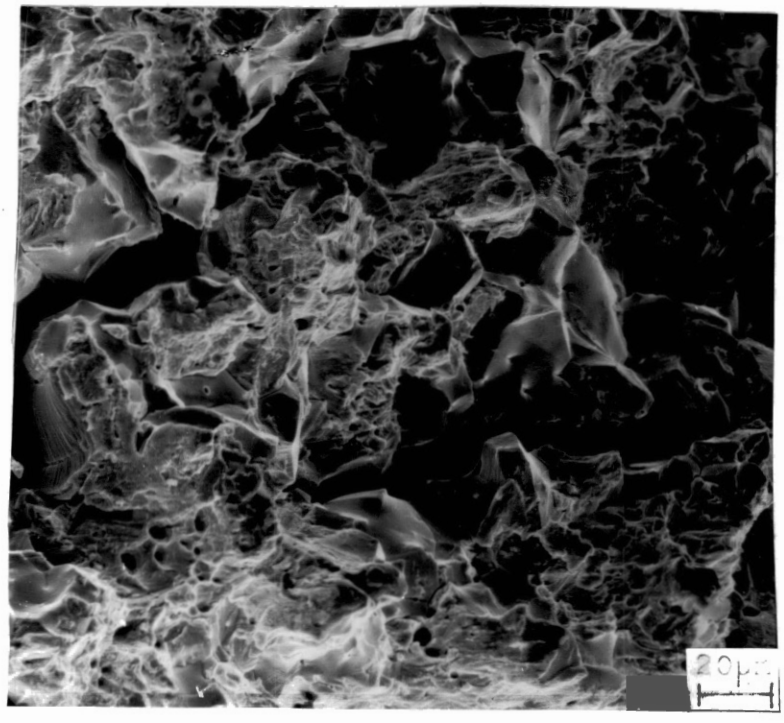
20μm

Figure 16. Non-microvoid type fracture surface that occurs in Inconel 625 around the outside edge of the specimen. The fracture mode changes quickly to microvoid, as seen in the lower right corner.

Figure 17. Part of a small area of non-microvoid type fracture surface that occurs on the outer edge of this Incoloy 825 fractured in hydrogen.

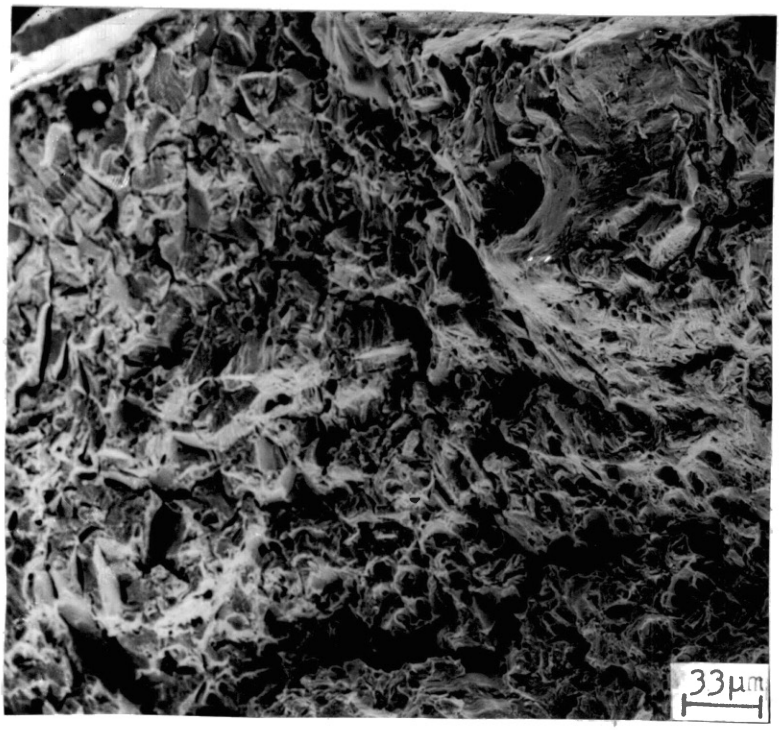
33μm

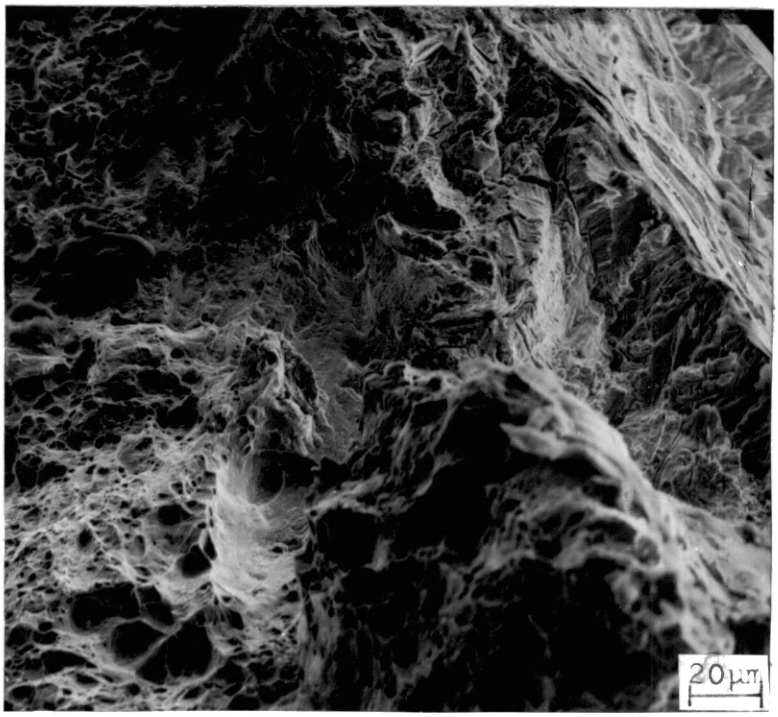
20μm

Nickel-Chromium-Iron Alloys. Incoloy 825 was the only alloy that gave a cup and cone type fracture and suffered the least loss of ductibility of any alloy tested. In the SEM, a very small rim of material, less than 2 grains deep did show signs of embrittlement in the form of crystallographic and non-crystallographic cracking (Figure 17).

3. Exploratory Fatigue Tests in Hydrogen

The fatigue tests in hydrogen were limited to Nickel 200, Monel 400 and Monel R405, Inconel 625 and Incoloy 825. The objective was to determine whether the behavior of hydrogen paralleled that of mercury. The fatigue lifetimes are compared in Table IV. In hydrogen, as in mercury, the fatigue lifetimes were all reduced. Nickel 200 was especially affected, as evidenced by the short fatigue life in hydrogen and a change in fracture mode from transgranular to intergranular (Figure 18). In the hydrogen environment under fatigue loading, Incoloy 825 showed the least reduction in life of all alloys under the SEM. The fatigue zone was only slightly affected by hydrogen (Figure 19). With the exception of Nickel 200 and Inconel 625, lives of all alloys in hydrogen were greater than the corresponding lives in mercury. Fractographically, the fatigue fractures were similar to the tensile fractures except that striations were sometimes seen in fatigue (Figure 20).

4. Determination of Significant Variables Using Nickel 200

Having established that all alloys are embrittled by hydrogen in a way broadly similar to mercury, Nickel 200 was chosen to perform specific tests to determine when the hydrogen was most active.

TABLE IV

FATIGUE DATA IN HYDROGEN
AND MERCURY

Alloy	Fatigue Life (10^3 Cycles)		
	Hydrogen	Mercury	Air
N02200	16	49	200
N04400	79	3.4	630
N04405	72	7	241
N06625	63	170	400
N08825	130	28	170

Figure 18. An intergranular fracture surface of Nickel 200 fatigued in hydrogen, near the origin.

Figure 19. The fatigue zone of an Incoloy 825 tested in hydrogen. The hydrogen apparently has little affect.

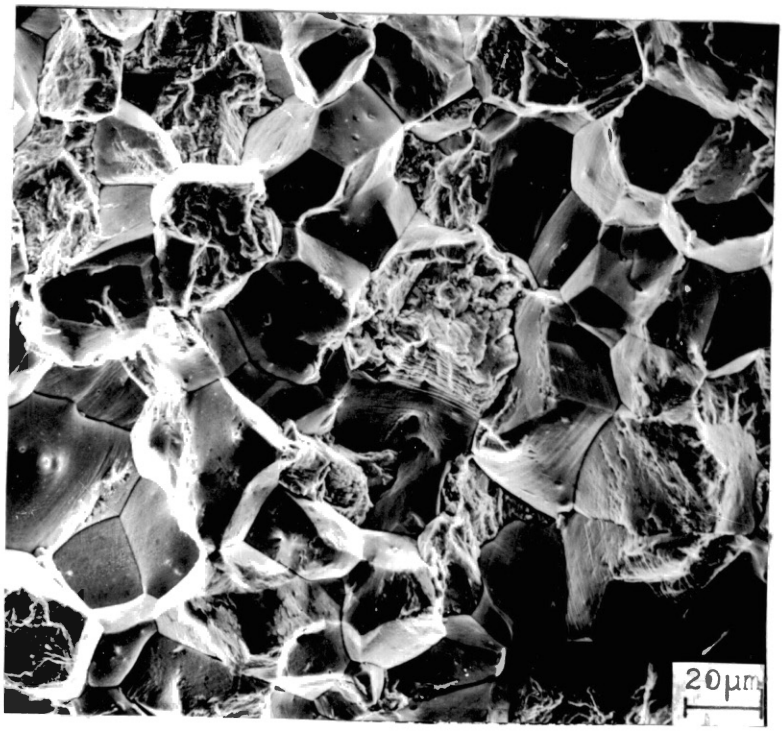
20μm

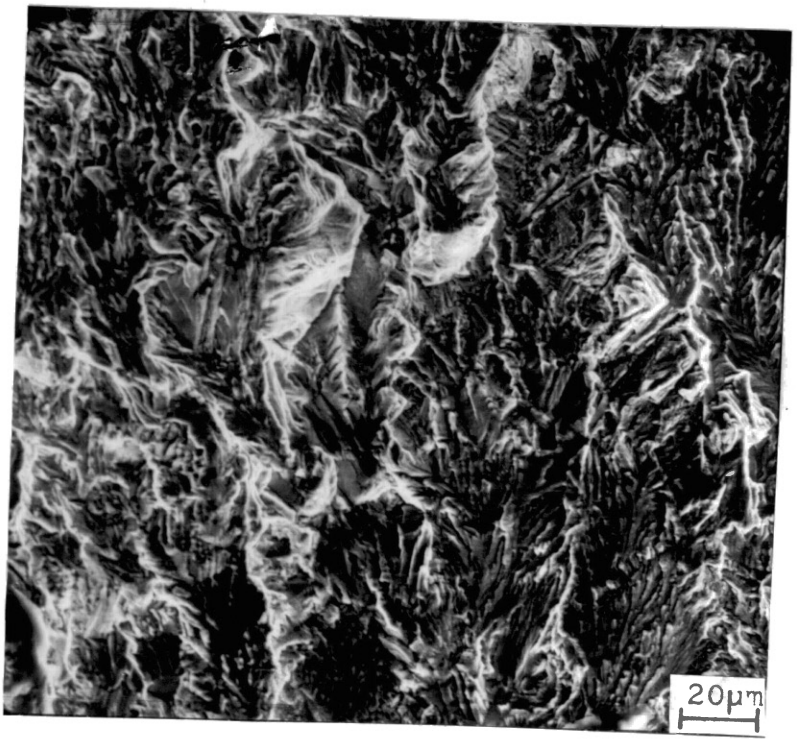
20μm

Figure 20. A rare patch of striations seen late in the fatigue zone of Nickel 200 tested in hydrogen.


20μm.

The Effect of the Charging Solution. A test was run with the solution around the specimen but no hydrogen charging whatsoever. As expected, the failure was cup and cone and indistinguishable from the test in air with a large reduction in area, as shown in Table V.

TABLE V

EFFECT OF CHARGING SOLUTIONS ON THE AMOUNT OF EMBRITTLEMENT

Environment	% Reduction in Area	Cup and Cone?
Air	85%	yes
Solution	86%	yes

The Effect of Charging Rate. The customary charging rate of 400 Am^{-2} had been selected based on literature studies.[15] That this was appropriate was determined by examining charging rates of 10 Am^{-2} to 2400 Am^{-2}. The results (Figure 21) show that at above charging rates of 400 Am^{-2} the extra hydrogen does not affect the amount of embrittlement. It is presumed that hydrogen saturation is occurring at the specimen surface and at crack tips.

The Effect of Precharging Time. Specimens were precharged for different lengths of time before testing, with the charging continued during

Figure 21. Variation of ductility with hydrogen charging rate for Nickel 200.

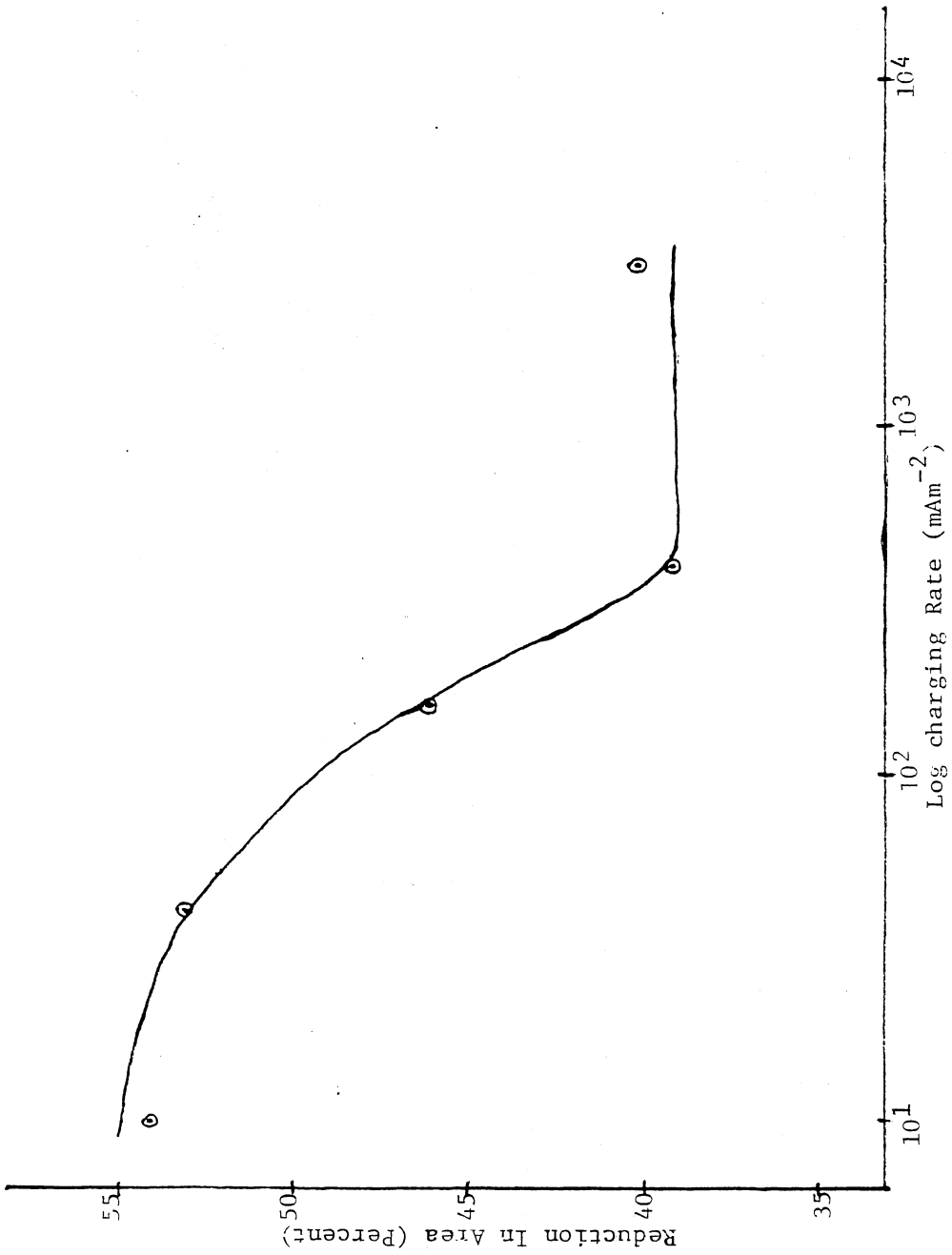
Reduction In Area (Percent)
55
50
45
40
35
10^1
10^2
10^3
10^4
Log charging Rate (mAm^{-2})

testing. Also, a specimen was precharged for three hours and then tested without charging during the test (no dynamic charging). The results, Table VI, show that precharging time was not an important variable and the absence of dynamic charging caused a cup and cone fracture that was not discernable from a fracture in air.

TABLE VI

THE EFFECT OF PRECHARGING
IN NICKEL 200

Precharging Time	% Reduction in Area	Cup and Cone?
2 hrs	39%	No
72 hrs	37%	No
3 hrs - Precharge only	85%	Yes

The Elimination of Precharging (Dynamic Charging Only). Some specimens were tested with no precharging and only dynamic charging, beginning when the stress reached the tensile strength of the nickel. It was found, Table VII, that embrittlement occurred even though the hydrogen was available to the specimen only in the last 38 minutes of a 3 hour test.

TABLE VII

COMPARISON OF PRECHARGED, DYNAMICALLY CHARGED, AND UNCHARGED SPECIMENS OF NICKEL 200

Condition	% Reduction in Area
Precharged + dynamically charged	39%
Dynamically charged at T. S. only	53%
No charging	85%

The Effect of Strain Rate. A ramp velocity of 7.6×10^{-4} mms^{-1} was used routinely. Experiments were performed at orders of magnitude different rates, the results of which are shown in Table VIII. At high strain rates, ($>7.6 \times 10^{-2}$ mms^{-1} ramp velocity) a cup and cone type fracture occurred in nickel 200, while at lower strain rates, ($<7.6 \times 10^{-3}$ mms^{-1} ramp velocity, a flat or slant fracture would occur. The lower the strain rate used, the more the embrittlement, as evidenced by a trend towards more intergranular fracture features and less reduction in area.

The strain rate also had a significant effect on the amount and type of side cracking as shown in Figure 22. At the higher strain rates, numerous cracks occurred 45° to the stress axis. When the strain rate was lowered, the 45° cracks disappeared and 90° to the stress axis

TABLE VIII

STRAIN RATE EFFECTS IN NICKEL 200

Ramp Velocity mm/sec	Environment	% Reduction in Area
7.6×10^{-2}	Hydrogen	62%
7.6×10^{-3}	Hydrogen	57%
7.6×10^{-4}	Hydrogen	54%
7.6×10^{-5}	Hydrogen	42%
7.6×10^{-4}	Mercury	63%
7.6×10^{-5}	Mercury	61%

cracks appeared. Lowering the strain rate still further caused a decrease in the number of 90° cracks and caused the remaining cracks to grow deeper.

5. Specific Tests and Measurements

Some specific tests and measurements were made because of matters arising from the previous section and from the published literature.

Microvoid Counts. One effect noticed by Thompson[34] is that hydrogen reduced the microvoid size of lower stacking fault energy (SFE) Inconel 625 more than the higher SFE Inconel 600 when fractured in hydrogen. He correlated the magnitude of the reduction of microvoid

a. 45° to the stress axis cracks that occur in Monel R405 tested with a high strain rate.

b. At a lower strain rate, the crack mode changes to 90° to the stress axis in Monel R405.

Figure 22. Side cracking that occurs in the hydrogen environment.

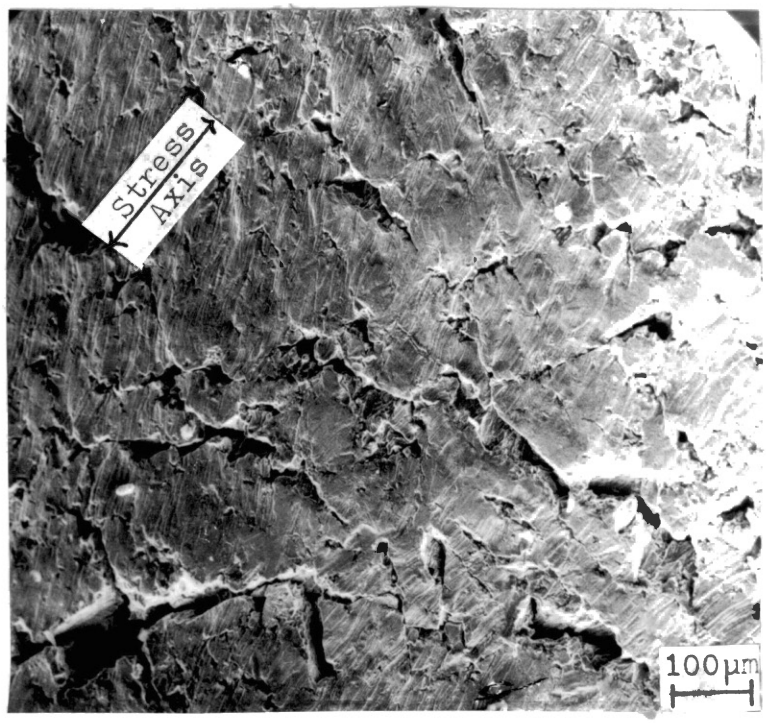
Stress
Axis
100μm

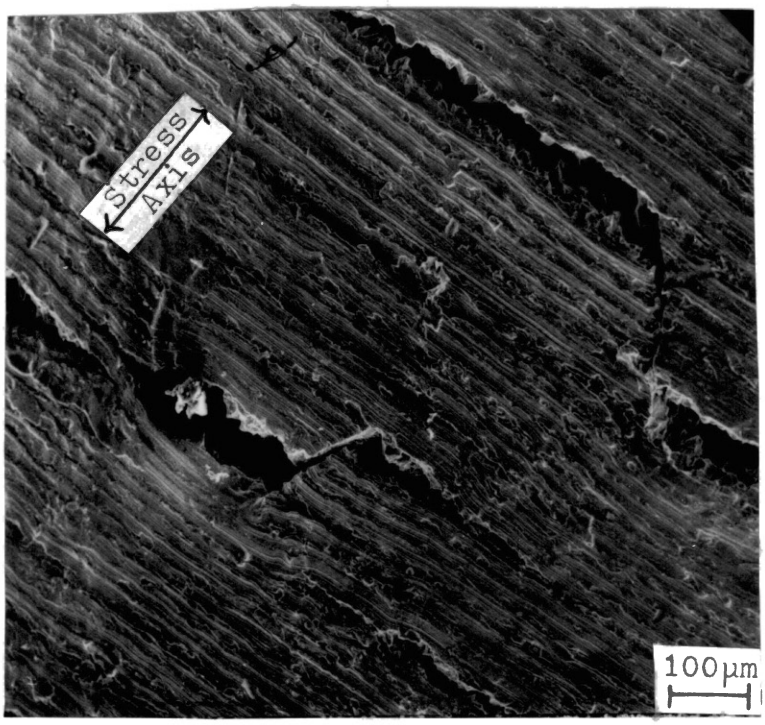
Stress
Axis
100μm

size to the amount of embrittlement and to a materials SFE. Because alloying elements decrease the SFE of nickel alloys[39] there should be a large SFE difference between Nickel 200 and Incoloy 825, with the other nickel alloys between these two. Nickel 200 and Inconel 625 were studied most extensively with Monel R405, 400 and Incoloy 825 providing additional data. Samples were tested in hydrogen, air and, in the case of Nickel 200, and Incoloy 625, mercury environments. Void counts were made, using transparent overlays, as described earlier. The fractures started from the outside (except Incoloy 825) but once the fracture mode transition to microvoid occurred, there was no systematic change in microvoid size over the remaining cross section. However, local areas could be found that had up to a factor of two difference in void count. In Nickel 200, there were clear differences in appearance between the hydrogen and air samples and in the mercury and air samples. The difference appeared to be a lack of coarse voids in the hydrogen and mercury environments. The void size for the cold worked material was smaller, but a similar trend was apparent. These observations were confirmed by measurements (Table IX) and by comparative photographs (Figure 23). In Incoloy 625, there was no visible difference in appearance between any of the states. (Figure 24). Measurements showed that the annealed material was effected very little by hydrogen while the cold worked material did show a small affect.

High Magnification Studies. Lynch[7] has done some experimental work involving high magnification SEM and TEM observations of intergranular fracture surfaces of hydrogen and mercury embrittled steels. His photographs showed voids of the order of 0.2 μm diameter on these

TABLE IX

COUNTS OF MICROVOID DIAMETERS FOR ANNEALED (AN) AND COLD WORKED (CW) SPECIMENS IN AIR (A), HYDROGEN (H) AND MERCURY (M) ENVIRONMENT, FOR AN AREA OF 0.01 MM^2

Alloy	Condition	Environment	Mean Count	Microvoids %		
				<5μm	5-10μm	>10μm
Nickel 200	AN	A	155	68	22	10
Nickel 200	AN	H	148	86	12	2
Nickel 200	CW	A	298	90	6	4
Nickel 200	CW	H	426	99	1	0
Inconel 625	AN	A	338	92	7	1
Inconel 625	AN	H	366	93	6	1
Inconel 625	CW	A	216	86	7	7
Inconel 625	CW	H	269	93	4	3
Monel 400	AN	A	137	67	16	17
Monel 400	AN	H	129	69	18	13
Incoloy 825	AN	A	233	90	6	4
Incoloy 825	AN	H	241	87	8	5
Nickel 200	AN	M	301	94	4	2

a. The microvoid size of a typical area of a Nickel 200 annealed specimen tested in air.

b. The microvoid size of a typical area of a Nickel 200 annealed specimen tested in hydrogen.

Figure 23. Results of the microvoid studies for Nickel 200.

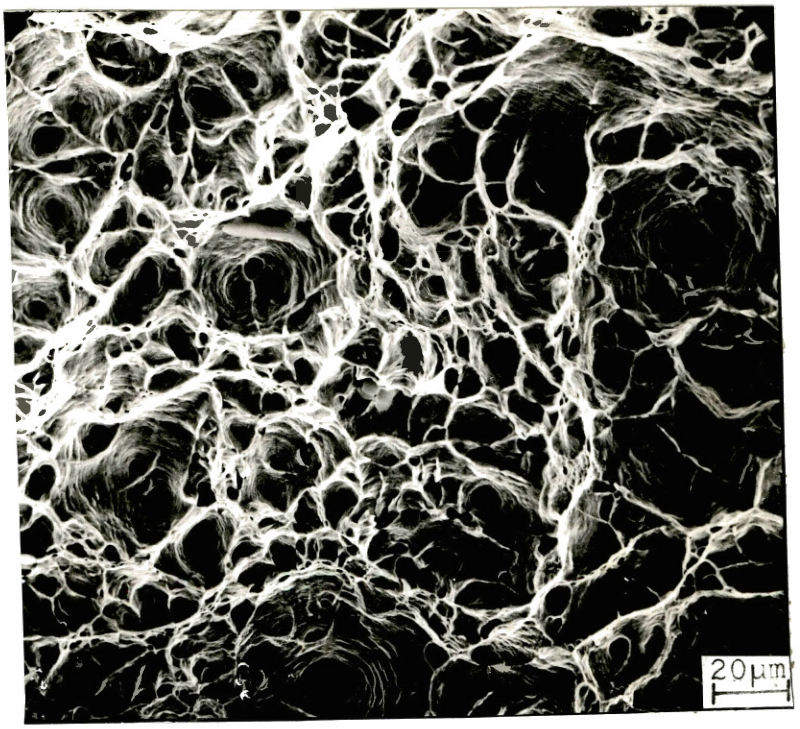
20μm

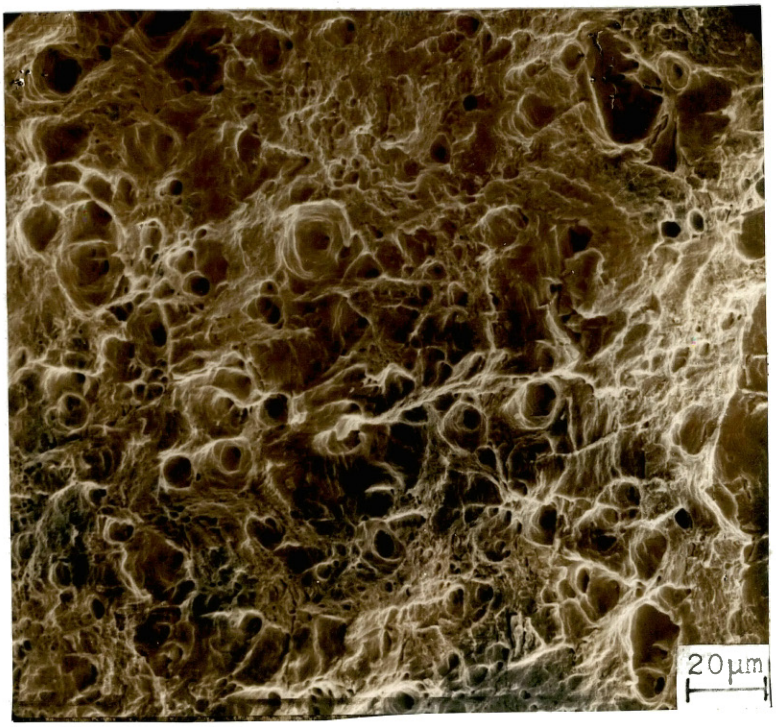
20μm

c. The microvoid size of a typical area of a Nickel 200 annealed specimen tested in mercury.

Figure 23. Continued.

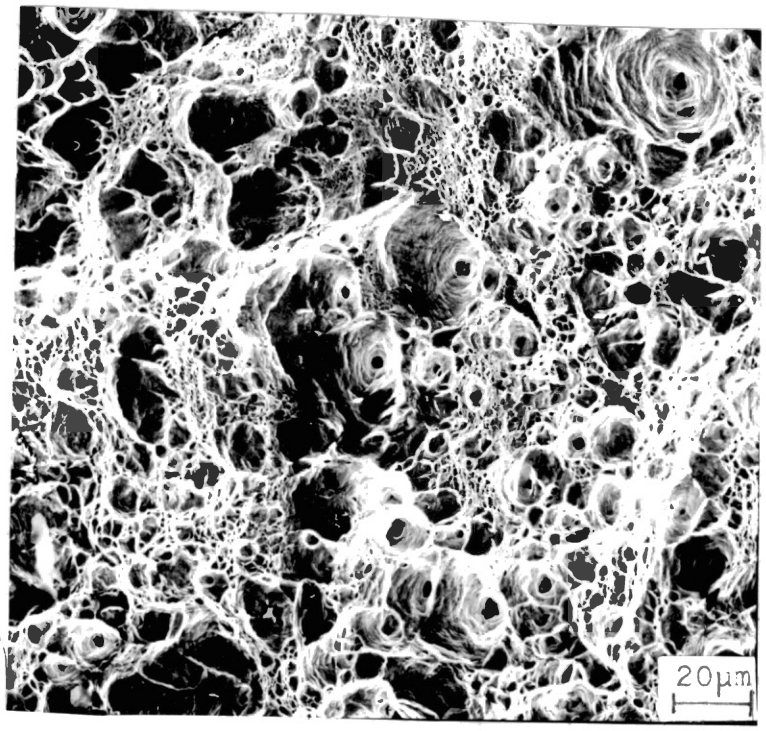
20μm

a. The microvoid size of a typical area of Inconel 625 annealed tested in air.

b. The microvoid size of a typical area of Inconel 625 annealed tested in hydrogen.

Figure 24. Results of the microvoid studies for Inconel 625.

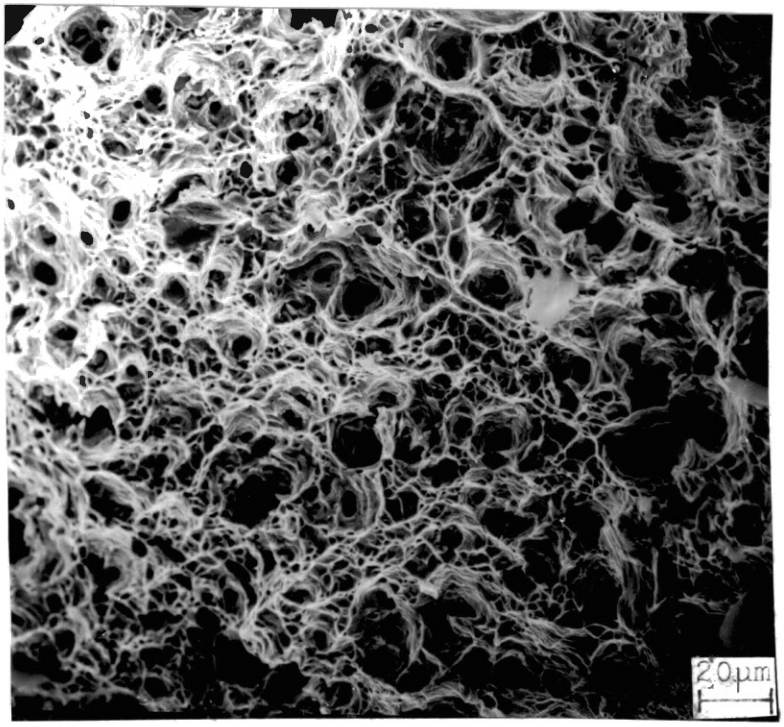
20μm

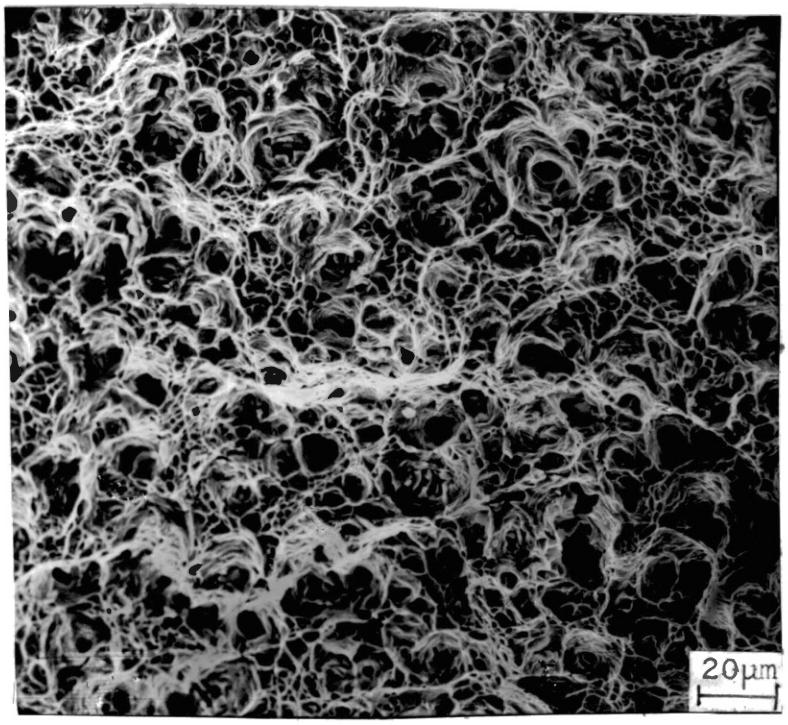
20μm

surfaces. An objective of this study is to determine if these voids appear on the intergranular fracture surfaces of the nickel alloys. An intergranular fracture surface of Monel 400 SSR tensile tested in hydrogen, a Nickel 200 fatigue tested in hydrogen and a Monel 400 SSR tensile tested in mercury were examined. As shown in the 5000 X SEM photographs in Figure 25, no microvoids appear in any photograph, although slip traces do appear. To determine if the slip traces are formed during the fracture process, both halves of a large grained Monel 400 sample, fractured in hydrogen, were examined. If the fracture surfaces looked the same, then the slip markings found were probably due to the fracture process, if not, the slip markings were formed after the surfaces separated. Both SSR tensile and fatigue loading were used. The fracture surfaces were matched and then examined in the SEM. The results, Figure 26, show that the transgranular fracture surfaces clearly do not have the exact same markings. The markings that do appear are on the same slip system but it is clear that much more slip exists on one half of the sample. Under fatigue loading, the surfaces matched nicely.

The Onset of Cracking. Because of the nature of the load control test, low strain rates occur before the tensile strength is reached, and high strain rates occur after. Because the strain rate is such an important variable, if hydrogen embrittlement occurred after necking, then a load control test would show very few embrittlement effects. Results from this study, Table X, show that a large reduction in area and few embrittlement effects occur in spite of the fact the standard test in hydrogen took about the same amount of time.

a. A high magnification view of an intergranular facet of Monel 400 SSR tensile tested in hydrogen.

b. A high magnification view of an intergranular facet of Nickel 200 fatigued in hydrogen.

Figure 25. High magnification photos of intergranular fracture surfaces.

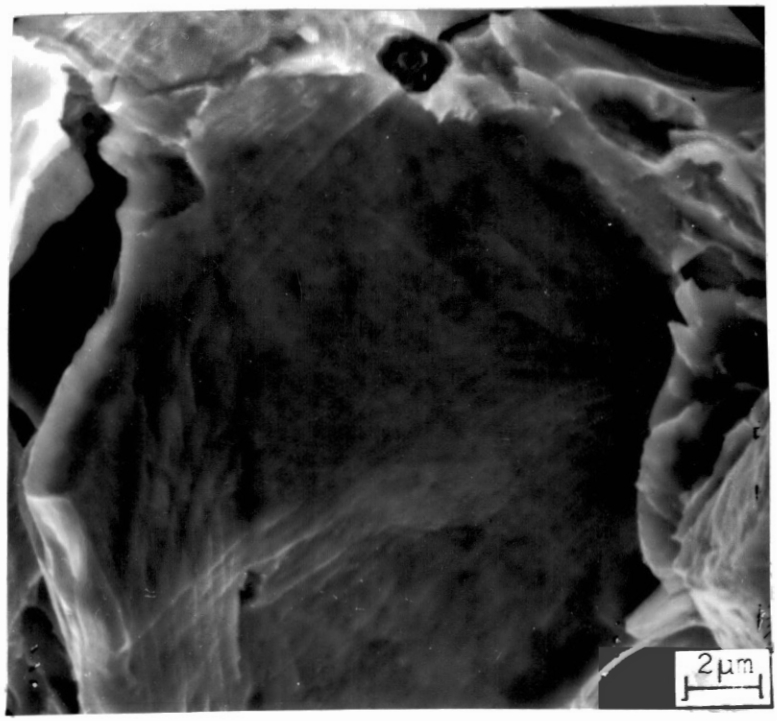
2μm

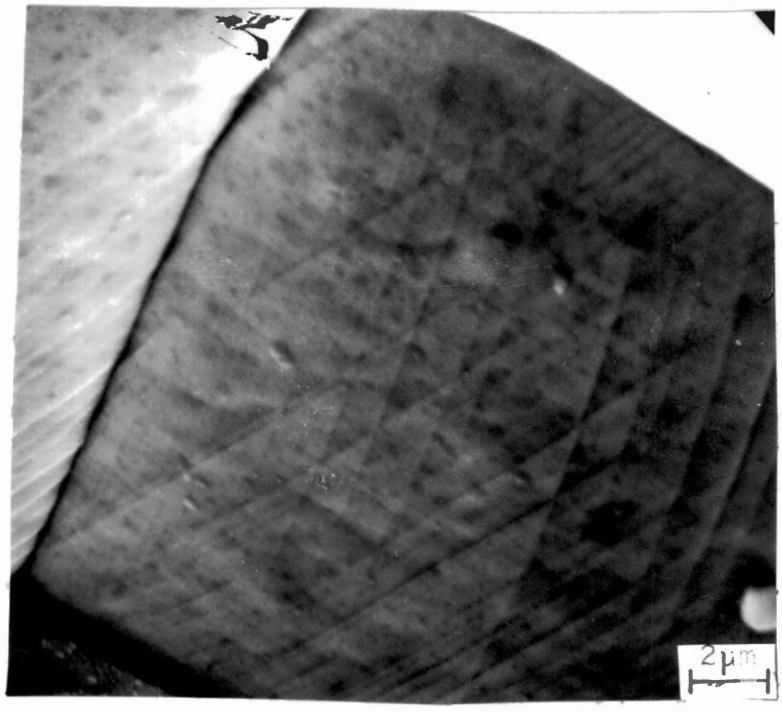
2μm

c. A high magnification view of an intergranular facet of Monel 400 SSR tensile tested in mercury.

Figure 25. Continued.

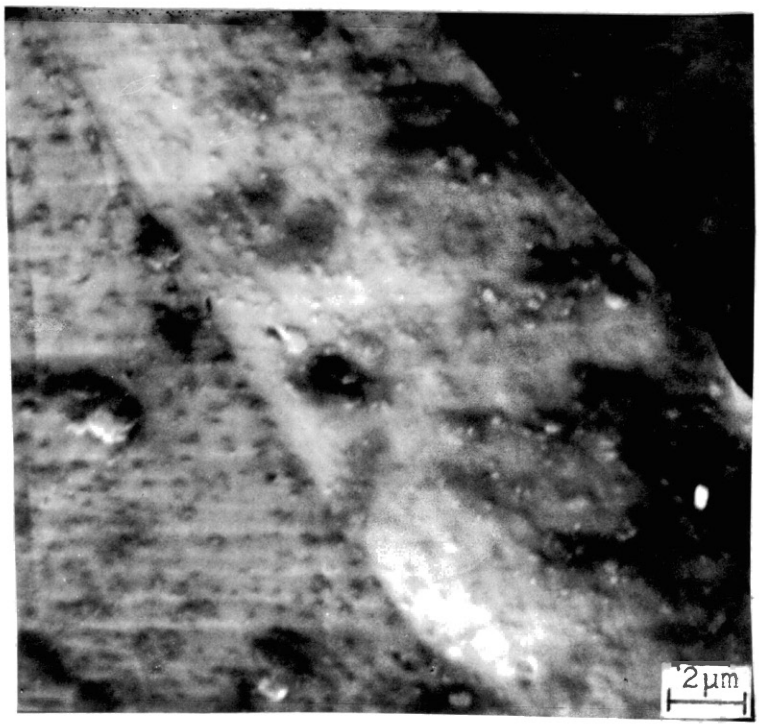
2μm

a. One half of a large grained Monel 400 SSR tensile tested in hydrogen.

b. The matching half of figure 26a in the exact same location, notice the two halves do not match.

Figure 26. Both halves of a large grained Monel, comparing matching fracture surfaces.

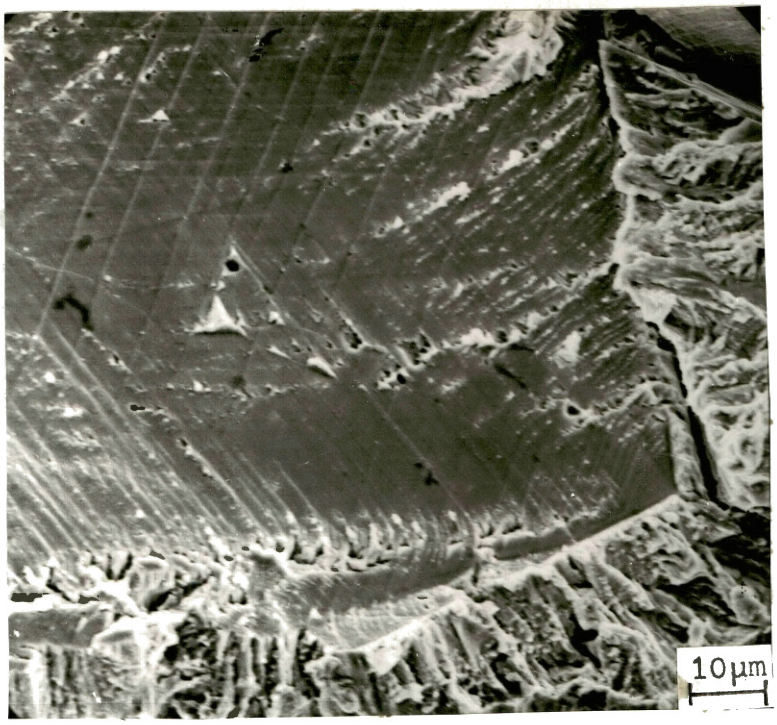
10μm

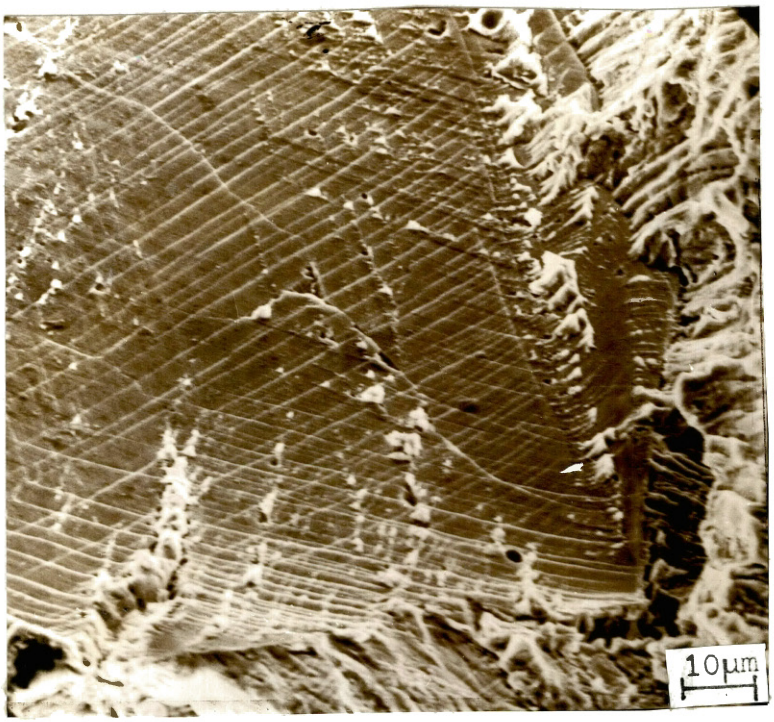
10μm

TABLE X

LOAD CONTROL TEST RESULTS

Test	% Reduction in Area	Cup and Cone?
Load Control in H_2	84%	Yes
Displacement Control in H_2	39%	No
Displacement Control in Air	85%	Yes

The next step was to test an annealed Nickel 200 in hydrogen under SSR tensile test conditions where the test was stopped periodically and the sample was inspected with a zoom microscope (10-70 power magnifications) for cracks. Then the precise time that detectable cracks form would be pinpointed. The results (Table XI) indicate that cracks become detectable between necking and failure.

TABLE XI

RESULTS OF CRACKING STUDIES
ON NICKEL 200

Elapsed Time (hr:min)	Stress (mPa)	Cracking?
:55	429	No
1:48	508	No
2:46	518	No
2:59	515	Yes
3:02	139	Yes
3:08	0	Fracture

The amount of time that elapsed between the detection of a crack and failure was only 9 minutes. Next, a sample of annealed Nickel 200 was tested in hydrogen under SSR conditions to the point at which cracks were first detected in the previous test. The sample was removed, sectioned and examined in the SEM. The photographs showed, Figure 27, that many cracks were formed but all are relatively small, extending at most, 5 or 6 grains along the surface. A closer examination shows that some of the cracks are transgranular and some are intergranular but all follow a path approximately perpendicular to the stress axis. Also, the cracks, as a rule, do not follow slip traces on the surface. A Nickel 200 annealed sample was then tested in air to the same point as the previous test, to determine if cracks develop on the outside surface. As shown in Figure 28 the outside surface did have many incipient cracks at this point. Although the cracks are much smaller than the cracks in hydrogen, they show the same general pattern.

Reference 41 shows that ductile microcracks do form on the outside surface of nickel alloys fractured in air. A striking resemblence to cracks formed in hydrogen is seen on the outside surface of a Hastelloy C-276 tensile tested in air (Figure 29). At this point, it was reasoned that if a crack could be formed on the outside surface of a specimen, that crack could grow in the hydrogen environment and cause failure before the tensile strength was reached. In an attempt to show this effect, two Nickel 200 specimens were fatigued in the solution, at a stress that gave a life of 200,000 cycles in air, for 4,000 and 40,000 cycles respectively. The load was removed, and a slow displacement ramp (7.6×10^{-4} mm/sec) was applied. It was thought that a fatigue crack would form on the specimen surface. However, no reduction in tensile strength

a. Cracks that occur on the outside surface of a Nickel 200 tested in hydrogen.

b. A closeup of Figure 27a showing that cracks do not tear across slip traces on grain boundaries.

Figure 27. Cracks that occur on the outside surface of a Nickel 200 specimen fractured in hydrogen.


50µm

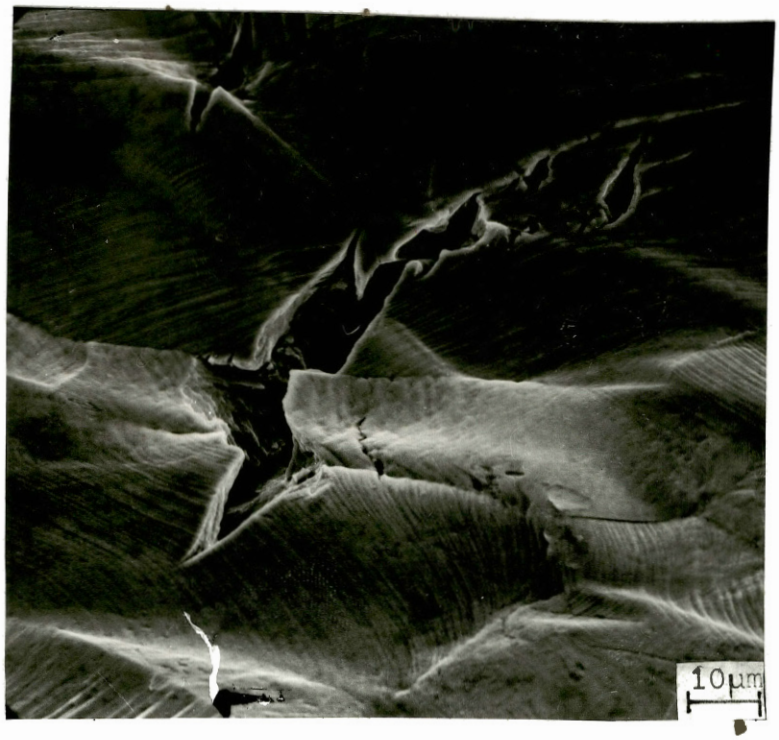
10µm

Figure 28. The outside surface of a Nickel 200 specimen, tested in air, showing incipient cracks.

Figure 29. The outside surface of a Hastelloy C-276 fractured in air showing 45° to the stress axis cracks.

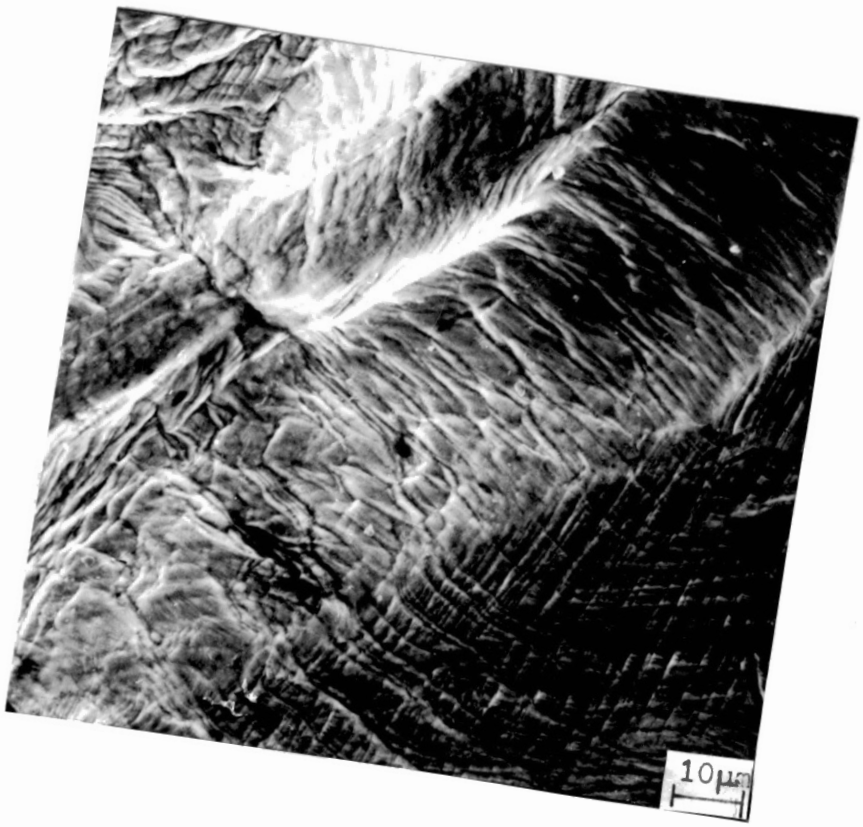
10μm


Stress
Axis
20μm

occurred. Next, a Monel 400 annealed specimen was tested using a different technique; it was fatigued for 40,000 cycles at a stress that gave a life of 600,000 cycles in air, but in the hydrogen environment. Without removing the load, a slow ramp (7.6×10^{-4} mm/sec) was applied. The specimen did show a slight drop in tensile strength (Table XII).

TABLE XII

FATIGUE-TENSILE TEST RESULTS

Material	Test	Reduction in area %	Tensile Strength (mPa)
Monel 400	SSR tensile in Hydrogen	12	571
Monel 400	Fatigue in H_2 tensile in H_2	14	529
Monel 400	Fatigue in H_2 tensile in air	68	629

B. Discussion

1. The Effect of Hydrogen on Crack Initiation and Propagation

Hydrogen embrittlement is caused by either easier crack initiation or enhanced crack propagation or both. If easier crack initiation were occurring, then cracks would appear earlier in the test than they would normally appear in air. The observation that hydrogen does not significantly affect the tensile strength of any alloy tested, suggests that no cracking occurs until after the tensile strength is reached. Load control tests done in this study are consistent with this suggestion.

Interrupted tensile tests have shown that detectable cracks occur only well after necking begins, and that cracks in air form at about the same point as cracks in hydrogen. Also, hydrogen is needed only after the tensile strength is reached to cause embrittlement. This indicates that cracks occur on the outside surface sometime after the tensile strength is reached, regardless of environment. The results of the cracking studies show that hydrogen does not cause detectable cracks to form earlier than they would in air, thus it can be argued that hydrogen does not affect crack initiation. The observation that the fatigue lives of all alloys are reduced in hydrogen, and other evidence in the literature discussed earlier, suggest that hydrogen very much increases fatigue crack growth rates. Other observations from this study show that cracks become detectable only 9 minutes before failure in a three hour SSR tensile test. This means that the crack grew from a detectable size to failure very quickly in proportion to the total lifetime. In air, cracks initiated on the outside surface but did not grow, failure occurred from the inside outward after much necking. In hydrogen, after microcracks initiated on the outside surface, they grew quickly, causing failures from the outside inward. Also, if cracks are formed below the tensile strength using fatigue, the cracks will grow when tested in SSR tension before the tensile strength is reached. This evidence suggests that once a crack is formed, the hydrogen enhances crack propagation.

2. Surface and Volume Effects in Hydrogen

Hydrogen embrittlement occurs in both steels and nickel alloys yet hydrogen diffusion rates in nickel alloys are orders of magnitude less

than in steel. The role of diffusion in hydrogen embrittlement is an important question. If hydrogen embrittlement is a volume effect, then diffusion rates matter very much because the hydrogen must diffuse through the material to cause embrittlement. If hydrogen embrittlement is a surface affect, then hydrogen need only be available at the crack tip surface to cause embrittlement, hence diffusion is unimportant but hydrogen availability and concentration would matter. Variables that effect hydrogen diffusion are amount of precharging and maybe stacking fault energy.[33] Variables that effect hydrogen concentration are dynamic charging rate and strain rate. The precharging tests show that the amount of precharging is not a significant variable, precharging alone will not cause embrittlement and applying the hydrogen at the tensile stress will cause embrittlement. The experimental results also show no direct connection between planar slip and the degree of embrittlement. For the concentration variables, however, the results show that strain rate, which is related to crack velocity, hence hydrogen concentration at the crack tip, and charging rate are significant variables. Moreover, hydrogen must be present during deformation and cracking in order to get embrittlement, as evidenced by the charging rate studies. All experimental evidence is consistent with hydrogen being a surface rather than a volume effect in nickel. Up to this point, it has been suggested that hydrogen effects crack propagation not crack initiation and that the hydrogen acts at the crack tip surface in a way that allows the crack to move through the metal easier. Two of the theories discussed earlier in the literature, the enhanced nucleation of dislocations and reduction in surface energy by absorption theories are consistent with the above observations. The only difference between the two theories

is the exact mechanism by which the absorbed hydrogen affects the crack tip. The enhanced nucleation of dislocations theory requires that all fractures in hydrogen be microscopically ductile. That is, all fracture surfaces, even the intergranular ones, be covered with microvoids. The findings of this study cannot confirm this for any intergranular fracture surface examined. Furthermore, the evidence suggests that slip bands formed on intergranular fracture surfaces occur after the surfaces separated, thus were not part of the fracture process. However, it is difficult to prove that microvoids do not exist on an undetectable scale and thus this theory cannot be ruled out but in the case of nickel alloys in hydrogen, the reduction in energy by absorption theory is most consistent with the experimental evidence.

3. Effect of Alloy Composition

One of the most important and interesting variables and the most difficult to explain is the affect of alloy composition. For example, according to Caskey,[40] in iron-chromium nickel alloys, the loss of reduction in area ranged from 0 to 97% depending on alloy composition. Clearly, this variable of composition strongly influences the extent of embrittlement. One proposed explanation is that the lower stacking fault energy hence more planar slip, causes more embrittlement. However, the results of this study show (Table XIII) that for the alloys tested, the higher alloy materials, thus those with lower SFE, gave the least amount of embrittlement. This result is quite opposite to that predicted by the slip planarity correlation. From the void counting studies, the inference is that any decrease in void size does not correlate well with SFE for the alloys tested. Furthermore, by directly

counting the voids, it can be seen that the total number of voids appears to be more or less constant between the air and hydrogen environment for a given state. This suggests that the same number of voids initiate in both environments (Table IX) but the number of large voids is smaller in the hydrogen environment. Thus the effect of hydrogen on voids may not be to promote void nucleation but to increase the growth of all voids. Looking at Table XIII it appears that the strain hardening coefficient gives a good correlation to the extent of embrittlement in this limited data. This could be due to the fact that the strain hardening coefficient is related to the amount of strain that occurs before necking. In a material with a large strain hardening coefficient, such as Incoloy 825, much strain occurs before necking and hence internal cracks may form and grow before external cracks develop. In materials such as Monel, with a lower strain hardening coefficient, cracking may develop externally before much straining occurs, thus leading to external crack growth early. Another explanation could be the effect of alloy composition on the chemiabsorption reaction, with some compositions absorbing hydrogen easily and others may be passivating and not absorbing as much hydrogen. Obviously, the effect of alloy composition is a complex issue, involving many variables such as SFE, strain hardening coefficient, alloy chemistry and surface film formation and cannot be explained easily.

4. Behavior of Nickel Alloys in Hydrogen as Related to Testing and Selection

In light of the testing of this study, several points of interest have arisen concerning testing and materials. It appears, by the

TABLE XIII

CORRELATION OF STACKING FAULT ENERGY, STRAIN HARDENING COEFFICIENT AND LOSS IN REDUCTION IN AREA AT FRACTURE

Alloy	% Loss In Reduction in Area	Strain Hardening Coefficient	SFE $ergCm^{-1}$
N04400	74	.24	54
N02200	54	.44	130
N06625	38	.58	33
N08825	1	.68	72

experimental results of this study, that hydrogen does not promote embrittlement until a crack forms and, in the SSR tensile test, cracks do not form until after necking. From the beginning of the test, until necking, there may be no difference between the hydrogen and the air environments. Therefore, a material with a high strain hardening coefficient will show a large amount of elongation before necking but be totally brittle after necking. Therefore, elongation at fracture includes the affect of the strain hardening coefficient as well as any embrittlement effects. The loss in reduction in area at necking takes more into account the events that occur after necking and is easy to measure accurately thus this is a non-subjective and desirable method of measurement. The reduction in average void size does take into account the events after necking but is more difficult to use and is more subjective. The fracture mode does not always correlate exactly to the loss in reduction in area but there is a correlation between the two. The change in fracture mode is the most subjective and difficult method of measuring embrittlement. However, for the data of this thesis, the loss of reduction in area and the fracture mode correlate with each other but not with the change in microvoid size (Table XIV). The fatigue life data for hydrogen, shown in Table IV also agree well with the above measurements that indicate Incoloy 825 was embrittled the least and Monel 400 the most. Many pitfalls exist, for example, the tensile strength in hydrogen in no way predicts the amount of embrittlement nor the fatigue life found in any alloy. Also the hydrogen charging rate and the strain rate can cause large changes in the extent of embrittlement. According to the literature, trace impurities can also cause large changes in the extent of embrittlement, so different heats

TABLE XIV

COMPARISON OF MEASUREMENT MODES

Alloy	% Loss In Reduction in Area	Extent at Fractographic Embrittlement	% Change In Void Size
N04400	74	Severe	6
N02200	54	Moderate	25
N06625	38	Slight	2
N08825	1	Very Slight	6

of the same alloy could have different properties, as related to hydrogen embrittlement.

5. A Comparison of the Behavior of Nickel Alloys in Hydrogen and Mercury

Of the many similarities that are apparent between hydrogen and mercury embrittlement, the fractographic similarities are the most obvious. In the SEM, under low magnification (500 X) the same features appear in the same order in both the hydrogen (Figure 13) and the mercury (Figure 10) environments. Under higher magnification, (5000 X) the intergranular fracture surfaces are also similar (Figure 25). The similarities occur in all alloys tested under a variety of conditions. The alloys also showed the same order of susceptibility to both environments with Monel 400 being the most susceptible and Incoloy 825 the least. The side cracking that occurs had the same appearance and both environments and had a similar shift from 45° to 90° cracking at lower strain rates (Figures 22 and 11). Both environments caused all alloys except Incoloy 825 to crack from the outside inward, in the SSR tensile test, giving a slant or flat fracture, that was very similar in appearance (Figures 7 and 12). The Incoloys gave the only cup and cone fractures in both environments. The hydrogen and the mercury also lowered the fatigue lives of all alloys but neither significantly lowered the tensile strength. Hydrogen and mercury had the same effect on the void size as shown in Table 9. This further reinforces the idea that hydrogen embrittlement is a surface effect, because the reduction in void size is so similar in the two different environments (Figure 23). Lowering the strain rate caused increased embrittlement in both environments, while

higher embrittler concentrations at the specimen surface also caused more embrittlement (Figures 3 and 4, Table IV). The fact is, fractures in both environments were so similar, they were difficult to tell apart. There is no phenonena occurring in hydrogen that does not occur in mercury. Lynch[7] and others[41] have compared hydrogen and liquid metal embrittlement of many alloy systems, including the nickel system and have concluded that all evidence is consistent with both having the same mechanism. If hydrogen and mercury embrittlement have the same mechanism for nickel alloys, and all evidence is consistent with this, then all theories based on diffusion and/or pressure mechanisms are not valid because mercury, as discussed earlier, does not diffuse into nickel alloys and will not create high pressures at voids. This supports the evidence already given that suggests that hydrogen embrittlement in nickel alloys is a surface effect.

CHAPTER V

CONCLUSIONS

With the reservation that only a limited (although representative) selection of nickel based alloys were tested, the following conclusions can be made.

1. Nickel and its alloys are all embrittled to some degree by hydrogen.

2. The hydrogen does not affect crack initiation.

3. The hydrogen does affect crack propagation rates.

4. The evidence is consistent with hydrogen embrittlement of these alloys being a surface rather than a volume effect.

5. Hydrogen and mercury embrittlement give similar fractographic features; differences between the two types of embrittlement are in the degree of embrittlement, with no consistent pattern apparent.

6. The reduction in surface energy by absorption best explains the experimental observations in both hydrogen and mercury.

7. The slip planarity correlation found in stainless steels, and the idea that hydrogen promotes increased void nucleation are not supported by the experimental evidence.

BIBLIOGRAPHY

1. Tuttle, R. N., R. D. Kane. Materials Performance, 22 (January, 1983), 9-10.

2. "Nickel Base Turbulars Tapped for Sour Wells." Metal Progress (October, 1982), 12.

3. Jewett, R. P. Corrosion (May, 1979), 151-160.

4. Laws, J. S., V. Frick and J. McConnell. "Hydrogen Gas Pressure Vessel Problems in the M-1 Facilities." NASA Report CR-1305, National Aeronautics and Space Administration, Washington, D.C., March, 1969.

5. Price, C. E., and J. K. Good. "Tensile Fracture Characteristics of Nickel, Monel, and Selected Superalloys Broken in Liquid Mercury," (submitted to the ASME Journal of Engineering Materials and Technology, 1982). Stillwater, Oklahoma: Oklahoma State University, College of Mechanical and Aerospace Engineering, 1982.

6. Hertzberg, R. W. Deformation and Fracture Mechanics of Engineering Materials. New York: John Wiley and Sons, 1976, pp. 378-400.

7. Lynch, S. P. Metals Forum, 2 (1979), 189-199.

8. Lynch, S. P. Scripta Metallurgica, 13 (1979), 1051-1056.

9. Speidel. M. O. Metallurgical Transactions, 6A (1975), 631.

10. I. M. Berstein and A. W. Thomson. Hydrogen Effects in Metals. Pennsylvania: The Metallurgical Society of AIME, 1981.

11. Shewman, P. G. "Hydrogen Attack of Carbon Steel." Effect of Hydrogen on Behavior of Materials. Eds. A. W. Thompson and I. M. Bernstein. New York: The Metallurgical Society of AIME, 1976, pp. 59-69.

12. Fiore, N. F. and J. A. Kargol. "Hydrogen-related Embrittlement of Ni-base Superalloys." International AIME Conference Proceedings, 1 (1981), 854.

13. Was, G. S., H. H. Tischner, R. M. Latinisoin, and R. M. Pelloux. Metallurgical Transactions, 12A (August, 1981), 1409-1418.

14. Beachem, C. D. Metallurgical Transactions, 3 (1972), 437.

15. Eastman, J, T. Matsumoto, N. Norita, F. Heubaum and H. K. Birnbaum. "Hydrogen Effects in Nickel -- Embrittlement or Enhanced Ductility?" International AIME Conference Proceedings, 1 (1981), 397.

16. Troian, A. R. Transactions ASM, 52 (1960), 54.

17. Oriani, R. A. and P. H. Josephic. Acta Met., 22 (1974), 1065.

18. Rice, J. R. and R. Thomson. Phil. Mag., 29 (1974), 73.

19. Funkenbusch, A. W., L. A. Heldt, and D. F. Stein. Metallurgical Transactions, 13A (April, 1982), 611-618.

20. Stein, D. F. Proceedings of the Third International Conference on the Strength of Metals and Alloys, (1973), 57. Cambridge, Eng,

21. Kamdar, M. H. Progress in Materials Science, 15 (1973), 289.

22. Price, C. E. "Introducing the Structural Materials of Modern Engineering." (Unpublished book used in Modern Materials class) Stillwater, Oklahoma: Oklahoma State University, College of Mechanical and Aerospace Engineering, 1974.

23. Lynch, S. P. "A Comparative Study of Stress-corrosion Cracking, Hydrogen-assisted Cracking and Liquid-metal Embrittlement in Al, Ni, Ti and Fe-based Alloys." International AIME Conference Proceedings, 1 (1981), 863.

24. Kamdar, M. H. Progress in Material Science, 15 (1973), 289-374.

25. Cornet, M., C. Bertrand, and M. DaChunha Belo. Metallurgical Transactions, 13A (January, 1982), 141-144.

26. Frandsen, J. D., W. L. Morris, and H. L. Marcus. "Fatigue Crack Propagation of a Nickel-Copper Alloy in Low Pressure Hydrogen." Hydrogen in Metals Proceedings of an International Conference on the Effects of Hydrogen on Materials, (September 23-27, 1973), 633-643.

27. Stoltz, R. E. and A. J. West. "Hydrogen Assisted Fracture in FCC Metals and Alloys." International AIME Conference Proceedings, 1 (1981), 541.

28. Kamdar, M. H. Phys. Stat. Solidi, 4 (1971), 225.

29. Price, C. E. and J. K. Good. "The Fatigue Behavior of Nickel, Monel and Selected Superalloys, Tested in Liquid Mercury and Air; A Comparison." (Unpublished research) Stillwater, Oklahoma: Oklahoma State University, College of Mechanical and Aerospace Engineering, 1982.

30. Coyle, R. J., Jr., J. A. Kargol, and N. F. Fiore. Metallurgical Transactions, 12A (April, 1981), 653-658.

31. Groeneveld, T. P. and A. R. Elsea. Hydrogen Embrittlement Testing. Philadelphia: American Society for Testing and Materials, 1972, pp. 18.

32. Latanison, R. M. and H. Apperhouser, Jr. Metallurgical Transactions, 5 (February, 1974), 483-492.

33. Thompson, A. W. and I. M. Bernstein. Advances in Corrosion Science and Technology. New York: Plenum, 1980, pp. 53-175.

34. Thompson, A. W. Scripta Metallugica, 16 (1982), 1189-1192.

35. Harris, I. R., I. L. Dillamore, R. E. Smallman, and B. E. P. Beeston. Phil. Mag., 14 (1966), 325-333.

36. Tegart, W. J. The Electrolytic and Chemical Polishing of Metals. Oxford, England: Pergaman Press Ltd., pp. 99-102.

37. Materials Testing System Operations Manual. 810/812 Series.

38. Model 173 Potentiostat, Galvanostat Operating and Service Manual. EG&G Princenton Applied Research, 1981.

39. Caskey, G. R., Jr. Microstructural Science, 9 (1981), 413-419.

40. Askok, S., N. S. Staloff, M. E. Glicksman, and T. Slavin. Scripta Metallurica, 15 (1981), 331-335.

41. Engel, L. and H. Klingele. An Atlas of Metal Damage. Engelwood Cliffs, New Jersey: Prentice-Hall, 1981, pp. 43.

42. Kotval, P. S. Metallography, 1 (1969), 261.

43. Harris, I. R., I. L. Dillamore. Phil. Mag., 11 (1966), 1331.

VITA[2]

Leland Bruce Traylor

Candidate for the Degree of

Master of Science

Thesis: A COMPARISON OF HYDROGEN AND MERCURY EMBRITTLEMENT OF NICKEL BASED ALLOYS

Major Field: Mechanical Engineering

Biographical:

Personal Data: Born in Livermore, California, May 11, 1960, the son of Mr. and Mrs. F. T. Traylor.

Education: Graduated from College High School, Bartlesville, Oklahoma, in May, 1978; received Bachelor of Science in Mechanical Engineering degree from Oklahoma State University in 1982; enrolled in the graduate program at Oklahoma State University in 1982; completed the requirements for Master of Science degree in July, 1983.

Professional Experience: Summer engineering trainee, TRW Reda Pump Company, 1979-1982; undergraduate and graduate teaching assistant, 1982-1983; engineer in training, 1982.